Assessing traffic disturbance, efficiency, and safety of the mixed traffic flow of Connected Vehicles and Traditional Vehicles by Considering Human Factors

AUTHORS

Anshuman Sharma[a], Zuduo Zheng[a,1], Jiwon Kim[a], Ashish Bhaskar[b], Md. Mazharul Haque[b]

[b]*School of Civil Engineering, The University of Queensland, St. Lucia 4072, Brisbane, Australia*
[c]*School of Civil Engineering and Built Environment, Science and Engineering Faculty, Queensland University of Technology (QUT), 2 George St, Brisbane, Qld. 4001, Australia*

ABSTRACT

In the foreseeable future, connected vehicles (CVs) will coexist with traditional vehicles (TVs) resulting in a complex mixed traffic environment and the success of CVs will depend on the characteristics of this mixed traffic. Therefore, before the large scale deployment of CVs, it is important to examine how CVs will influence the characteristics of the resultant mixed traffic. To achieve this aim, this study models the mixed traffic of TVs and CVs, and examines the traffic flow disturbance, efficiency, and safety. Intelligent Driver Model (IDM) with estimation errors is utilised to model TVs since it incorporates human factors such as estimation errors. Whereas, connected vehicle driving strategy integrated with IDM is utilised to model CVs because it incorporates driver compliance, a critical human factor for the success of CVs. Moreover, two classes of drivers based on their compliance levels are considered, namely the high-compliance drivers and the low-compliance drivers, to comprehensively investigate the impact of driver compliance on the mixed traffic of CVs and TVs. Two simulation experiments are performed in this study. The first experiment is used to measure traffic flow disturbance and safety while the second is used to measure the traffic flow efficiency. Furthermore, a total of 7 mixed traffic environments are generated in each experiment via different combinations of TVs, CVs with low compliance drivers, and CVs with high compliance drivers. Another important point considered in the simulation is the spatially distribution of CVs in the platoon. As such, three platoon policies are investigated. In the first policy i.e., the best case, the CVs are spatially arranged with a motive to maximise benefits from CVs whereas in the second policy i.e., the worst case, the CVs are spatially arranged with a motive to minimise benefits from CVs. Finally, in the third platoon policy i.e., the random case, the CVs are distributed randomly in the platoon. This study demonstrates the importance of the spatial arrangement of CVs in a platoon at a given penetration rate and its impact on traffic flow disturbance, efficiency, and safety. Moreover, findings from this study underscores that CVs can supress the traffic flow disturbance, and enhance traffic flow efficiency, and safety; however, traffic

[1]Corresponding author. Tel.: +61 7 3443 1371
E-mail address: zuduo.zheng@uq.edu.au (Z. Zheng)

engineers and policy makers have to be cautious regarding how CVs are distributed in a traffic stream when deploying these vehicles in the real world traffic environment.

1. INTRODUCTION AND LITERATURE REVIEW

Connected vehicles (CVs) are the vehicles equipped to provide surrounding traffic information to drivers via vehicle-to-vehicle and vehicle-to-infrastructure, or vehicle-to-everything communications. Vehicle-to-everything communication includes vehicles, infrastructure, pedestrians, aftermarket devices, and any entity that may affect the CVs' dynamics. Note that this study considers manually driven CVs. The key advantages of CVs include enhancing traffic efficiency by alleviating traffic congestion, improving traffic safety, and reducing traffic emissions (Kim, 2015). For the foreseeable future, CVs will need to co-exist with traditional vehicles (TVs) (i.e., the present-day vehicles without communication capabilities and without driver assistance) in a mixed traffic environment and the characteristics of this mixed traffic will govern achieving the potential benefits of CVs. The resultant mixed traffic flow of CVs and TVs will have complex characteristics because of the differences in vehicular dynamics of CVs and TVs. Adding to the complexity are the human drivers controlling CVs and TVs. This study focusses on the microscopic modelling of the mixed traffic of CVs and TVs with a focus on human factors, and investigates the impact of CVs on traffic flow disturbance, efficiency, and safety in the mixed traffic environment. The amplitude and duration of traffic oscillations are utilised as the measures of traffic flow disturbance, and modified time-to-collision and deceleration rate to avoid the crash as the measures of traffic safety. Moreover, This study computes the average flow and the average speed of the mixed traffic using Edie's method (Edie, 1963) as measures of traffic efficiency.

Current research on mixed traffic modelling has focused on the mixed traffic of connected and automated vehicles (CAVs) and TVs (e.g., Fernandes and Nunes, 2012; Ghiasi et al., 2017; Gong and Du, 2018; Jia et al., 2019; Jia and Ngoduy, 2016; Jiang et al., 2017; Rios-Torres and Malikopoulos, 2018; Ye and Yamamoto, 2018; Zhao et al., 2018), automated vehicles and TVs (Bhavsar et al., 2017; Calvert et al., 2020; D. Chen et al., 2017; Z. Chen et al., 2017; Levin and Boyles, 2016; Rao and Varaiya, 1993; Talebpour et al., 2017; van den Berg and Verhoef, 2016), other intelligent vehicles (adaptive cruise control (ACC) or cooperative adaptive cruise control (CACC))[1] and TVs (Arem et al., 2006; Arnaout and Arnaout, 2014; Jerath and Brennan, 2012; Kesting et al., 2008; Liu et al., 2018; Ngoduy, 2012; Schakel et al., 2010; Shladover et al., 2012; Vander Werf et al., 2002; Wang et al., 2016, 2013), CVs, TVs, and automated vehicles (e.g., Ni et al., 2011; Talebpour and Mahmassani, 2016), and CVs and TVs (e.g., Guériau et al., 2016; Talebpour et al., 2016; Talebpour and Mahmassani, 2016; Xie et al., 2018; Zhu and Ukkusuri, 2017, 2016). Modelling the mixed traffic of CVs and TVs using simulation packages is another embraced approach other than analytical modelling due to the ease of model development and the flexibility to test models in various futuristic traffic conditions. The traffic simulation packages such as VISSIM, AIMSUN, PARAMICS, SUMO, etc., are sometimes integrated with the network simulation packages such as ns-2, OMNET++, etc., to model the

[1] ACC and CACC can be treated as an AV and CAV with Level 1 automation.

mixed traffic (Kim, 2015; Olia et al., 2016; Rahman et al., 2018; Rahman and Abdel-Aty, 2018; Sommer et al., 2011). Henceforth, the term mixed traffic represents the mixed traffic of CVs and TVs.

Through the analytical modelling and numerical simulation of the mixed traffic, Ni et al. (2011) modified the reaction time parameter of the Gipps' car-following model (Gipps, 1981) to distinguish between TVs and CVs, and showed that with the increase in the market penetration rates of CVs, the lane capacity increases. Talebpour and Mahmassani (2016) employed a prospect theory based car-following model (Talebpour et al., 2011) and Intelligent Driver Model (IDM) (Treiber et al., 2000) to model car-following behaviour of TVs and CVs in the mixed traffic, respectively. They reported suppressed oscillations, fewer collisions, and increased throughput as the market penetration of CVs was increased in the mixed traffic. Zhu and Ukkusuri (2016) considered Newell's car-following model (Newell, 2002) to update car-following states of CVs and TVs in the mixed traffic, and reported enhanced mobility benefits (in terms of both total travel time and distance) with increasing market penetration rates of CVs. Recently, Xie et al. (2018) have modified IDM based on a generic car-following model framework for TVs and CVs, and have demonstrated similar benefits of CVs in the mixed traffic environment.

A major limitation of the aforementioned studies is the models utilised to simulate car-following behaviour of CVs. The models considered assume that the drivers fully comply with the information provided and thus, they completely ignore a critical human factor—the driver compliance. In the case of CVs, drivers receive critical information such as the position and the speed of the leader, the space gap to the leader, upcoming safety critical situations, any traffic incident at the downstream, etc., and it is at drivers' discretion whether they comply with the information or not. Note that if drivers decide to ignore the information, all the advantages of CVs will be nullified. Therefore, driver compliance is a critical factor to incorporate when modelling the microscopic characteristics of CVs in the mixed traffic environment (Sharma et al., 2017).

Moreover, almost all the studies except Talebpour and Mahmassani (2016) ignored driver errors such as perception and estimation errors when modelling car-following behaviour of TVs. The role of human drivers in controlling TVs is equally important since drivers take operational (steering, acceleration/deceleration, monitoring, and braking), tactical (lane-changing, responding to a sudden event, deliberately driving slow or fast etc.), and strategic (origin-destination points etc.) decisions throughout the course of driving. However, due to limited perception, anticipation, and judgement capabilities drivers are bound to make errors that can jeopardize traffic efficiency and more importantly traffic safety. Hence, driver errors shall be incorporated when modelling the microscopic characteristics of TVs in the mixed traffic environment (Sharma et al., 2017; Treiber et al., 2006). These deficiencies in modelling car-following behaviour of TVs and CVs can cause underestimation or overestimation of the potential benefits of CVs.

Another major limitation is that the previous studies overlooked the distribution of CVs in a platoon i.e., the spatial arrangement of CVs from head to tail of a platoon when investigating the impact of the penetration rate of CVs on traffic flow efficiency, and safety. Note that CVs

have only communication capabilities and are not equipped with sensing technologies such as cameras, RADAR, LiDAR, etc., to gather information about TVs. Thus, CVs can only receive information from other CVs, and in car-following scenarios the information will be useful only when the leading vehicle is a CV. This study demonstrates that an inefficient arrangement of CVs in a platoon can challenge the consensus among previous studies that traffic flow efficiency, and safety always increase with an increase in the penetration rate of CVs.

Motivated by the limitations and gaps mentioned above, in this study, IDM with estimation errors is considered to simulate car-following behaviour of TVs whereas connected vehicle driving strategy integrated (CVDS) with IDM i.e., CVDS-IDM (Sharma et al., 2019b) is adopted to simulate car-following behaviour of CVs. CVDS-IDM explicitly incorporates driver compliance behaviour, which is modelled using Prospect theory (Kahneman and Tversky, 1979). Liu et al. (2017) did propose a methodology that incorporated the ADAS-affected driving behaviour modelling (driver compliance, perception reaction time, and ADAS influence). Driver compliance as per Liu et al. (2017) was modelled as a random number whereas in the case of CVDS-IDM the driver compliance modelling was based on theoretically, behaviourally, and practically sound prospect theory. To comprehensively investigate the impact of driver compliance on the mixed traffic, two classes of drivers based on compliance levels are considered, namely the high-compliance drivers and the low-compliance drivers. Furthermore, three platoon policies characterised by different spatial arrangements are defined and analysed to understand the impact of spatial arrangements of CVs in the mixed traffic platoon on traffic flow disturbance, efficiency, and safety. The first platoon policy attempts to maximise the benefits of CVs via an efficient arrangement of CVs in a platoon whereas the second platoon policy minimises the benefits of CVs via an inefficient arrangement of CVs in a platoon. The third platoon policy considers the random arrangement of CVs in the platoon. The traffic flow disturbance, efficiency, and safety are evaluated for the three platoon policies and for different penetration rates of CVs in the mixed traffic environment.

The remainder of the paper is organised as follows. Section 2 details car-following models employed to model TVs and CVs. The indicators of traffic flow disturbance, efficiency, and safety and how to calculate these indicators using trajectory data are described in Section 3. Section 4 details the experiment design and the scenarios considered for the analysis in this study. Section 5 presents results and findings from the analysis. Section 6 discusses the implications of this study, and finally, Section 7 summarizes the main conclusions and suggests future research directions.

2. CAR-FOLLOWING MODELS CONSIDERED IN THIS STUDY

2.1 Intelligent Driver Model with estimation errors

The intelligent driver model (IDM) with estimation errors is employed to model car-following behaviour of TVs. IDM belongs to the category of desired measures models (Saifuzzaman and Zheng, 2014) and assumes that the acceleration is a continuous function of driver's speed, spacing to the leader, and speed difference between the leader and the follower. Equations (1)

and (2) present the mathematical formulation of the IDM acceleration function of the nth driver.

$$a_n(S_n, V_n, \Delta V_n) = a\left[1 - \left(\frac{V_n}{V_0}\right)^{\delta} - \left(\frac{s^*(V_n, \Delta V_n)}{S_n}\right)^2\right] \quad (1)$$

$$s^*(V_n, \Delta V_n) = s_0 + \max(0, TV_n + \frac{V_n \Delta V_n}{2\sqrt{ab}}) \quad (2)$$

where V_0, δ, T, s_0, a, and b are desired speed of the vehicle (m/s), free acceleration exponent, desired time gap (s), standstill distance (m), maximum acceleration (m/s^2), and desired deceleration of vehicle (m/s^2), respectively. Also, a_n is the IDM acceleration (m/s^2), s^* is the desired spacing (m), V_n is the speed(m/s), ΔV_n is the relative speed (difference of the follower's speed V_n and the leader's speed (V_{n-1}))(m/s), and S_n is the space gap (m).

2.1.1 Incorporating estimation errors in IDM

Drivers make errors when estimating stimuli associated with the leader such as changes in space gap and speed of the leader. Moreover, drivers react differently at different times to the same stimuli i.e., the existence of the intra-driver heterogeneity (Ossen and Hoogendoorn, 2011). For instance, for the same stimulus, a driver can commit different magnitudes of the estimation errors at different times. Therefore, time-dependent estimations errors are included in the space gap parameter and the leader's speed parameter of the original IDM model. This study incorporates the estimation errors in IDM as per Treiber et al. (2006) and Treiber and Kesting (2013), and according to these studies estimation errors are taken into account by modelling them as a Wiener process. The estimated space gap is calculated as per Equation (3):

$$S_n^{est} = S_n\, e^{V_s w_s(t)} \quad (3)$$

where S^{est} is the estimated space gap by the driver, S_n is the actual space gap, V_s is the coefficient of variation and describes the relative standard deviation of S_n^{est} from the true value S_n, and $w_s(t)$ is the Wiener process which describes the temporal evolution of errors in space gap. The estimated leader's speed and the corresponding relative speed are presented in Equations (4) and (5):

$$V_{n-1}^{est} = V_{n-1} - s\sigma_r w_l(t) \quad (4)$$

$$\Delta V_n^{est} = \Delta V_n + s\sigma_r w_l(t) \quad (5)$$

here V_{n-1}^{est} is the estimated leader's speed, V_{n-1} is the actual leader's speed, σ_r is the constant standard deviation of the relative approach rate, and $w_l(t)$ is similar to $w_s(t)$ and describes the temporal evolution of errors in leader's speed. The revised model is termed as Human IDM (HIDM) in this study. Other variants and advancements of HIDM are also available in the literature (Gu and Saberi, 2019; Jia and Ngoduy, 2016; van Lint and Calvert, 2018). When estimating the HIDM acceleration, S_n and ΔV_n are replaced by S_n^{est} and ΔV_n^{est} respectively, in the original IDM model. The value of $w_s(t)$ or $w_l(t)$ at the i^{th} iteration (w_i) is given by Equation (6):

$$w_i = e^{\frac{-\Delta t}{\tilde{\tau}}} w_{i-1} + \sqrt{\frac{2\Delta t}{\tilde{\tau}}}\eta_i \quad (6)$$

where η_i are computer-generated i.i.d. pseudo-random numbers following the uniform distribution with expectation zero and unit variance, $w_0 = \eta_0$, Δt is the time step, and $\tilde{\tau}$ is the persistence or correlation time. As per Treiber and Kesting (2013) "…if a driver, say, underestimates the gap at a given time, he or she is likely to underestimate it in the next second as well. In mathematical terms, the errors at two times are positively correlated for small time differences of a few seconds up to one minute." Thus, the persistence time is the time period within which the estimation errors are correlated.

2.2 Connected vehicle driving strategy (CVDS) integrated with IDM

Sharma et al. (2019b) formulated CVDS to explicitly model the driver compliance to the continuous information and the advanced event-triggered information. The information that is always present on the windscreen or driver assistance devices is called the continuous information whereas the information that is delivered to drivers a few seconds before the occurrence of an event is called the advanced event-triggered information. The advanced event-triggered information is possible assuming that the connectivity technologies will be smart enough to warn the drivers about the critical events in advance. The continuous information can include the speed of and the spacing to the leader whereas the advanced event-triggered information can include the warning messages such as 'leader braking hard' that is delivered to the follower a few seconds (e.g., around 3 s) before the leader brakes. The detailed information on this driving simulator experiment can be found in Ali et al. (2020).

CVDS is a general driving strategy that can be integrated with any existing car-following models to describe the connected vehicle car-following behaviour. Moreover, CVDS has two components: (a) part I incorporates the impact of continuous information into the model; and (b) part II incorporates the impact of the advanced event-triggered information (currently limited to modelling the hard braking cases only). The driver compliance in CVDS is modelled using prospect theory (Kahneman and Tversky, 1979) and it is an integral element of both the parts.

2.2.1 CVDS Part I: Modelling the driver's response to the continuous information

When modelling the driver response to the continuous information, the stimuli i.e., the relative speed and the spacing are considered as estimation error free since connected environment provides such information to drivers. Obviously, the assumption here is that drivers devote their undivided attention to such information. As per Sharma et al. (2019b), the time gap parameter in car-following models is multiplied with $(1 + UT(h_{obs}))$ to accommodate the impact of driver compliance on the connected vehicle car-following behaviour.

The mathematical formulations of CVDS-IDM part I are presented in Equations (7) and (8):

$$a_n(S_n, V_n, \Delta V_n) = a\left[1 - \left(\frac{V_n}{V_0}\right)^{\delta} - \left(\frac{s^*(V_n, \Delta V_n)}{S_n}\right)^2\right] \quad (7)$$

$$s^*(V_n, \Delta V_n) = s_0 + (1 + UT(h_{obs}))TV_n + \frac{V_n \Delta V_n}{2\sqrt{ab}} \quad (8)$$

where, $UT(h_{obs})$ is the utility value calculated at h_{obs} using prospect theory shape parameters α, γ, and λ. The parameter h_{obs} is the observed headway between the follower and the leader measured at the time when the messages are received by the followers. In the case of continuous information, the h_{obs} is measured at each time since messages are available all the time. Refer to Sharma et al. (2019b) for a detailed discussion on how $UT(h_{obs})$ is evaluated using prospect theory.

The compliance is measured in terms of driver's response to a message and categorises compliance into two levels, namely the high compliance and the low compliance. At each time instance, a driver can comply either at a high level or a low level depending on h_{obs} at the time of the message display. Other human factors that can contribute to choosing a particular compliance level are trust in the connected vehicle technology, driving behaviour, and the type of message (e.g., a warning message, an advisory message, etc.). In response to a continuous message such as the speed of and the spacing to the leader, a high compliance driver will maintain a large headway and low acceleration noise as compared to a low compliance driver. Numerically, a high/low $UT(h_{obs})$ value indicates a high/low compliance drivers. Figure 1 displays the usefulness curves for high compliance and low compliance drivers. These curves are developed using the formulation $V\ (h_{obs}) = \frac{1}{(1+e^{\lambda(\alpha h_{obs}-1)})}$. The figure depicts that the high compliance drivers predominantly have a high usefulness value for a majority of h_{obs} whereas the low compliance drivers predominantly have a low usefulness value for a majority of h_{obs}. Here, a usefulness value ($V(h_{obs})$) shows how useful a message is to a driver depending upon the h_{obs}.

Note that this study only considers the continuous information and its impact on car-following behaviour in connected environment. Thus, this study integrates CVDS part I with the IDM model to simulate car-following behaviour of CVs in the presence of continuous information. For part II of CVDS and its integration with a car-following model refer to Sharma et al. (2019b). Moreover, CVDS-IDM was rigorously calibrated using connected vehicle trajectory data obtained from the driving simulator. The average fitting errors were 13.3% which is consistent with typical calibration error range reported in the literature. In addition to calibration, the numerical and behavioural soundness of the model was also examined, and it was found that CVDS-IDM is superior to IDM. Thus, CVDS-IDM can reproduce the connected vehicle car-following behaviour successfully.

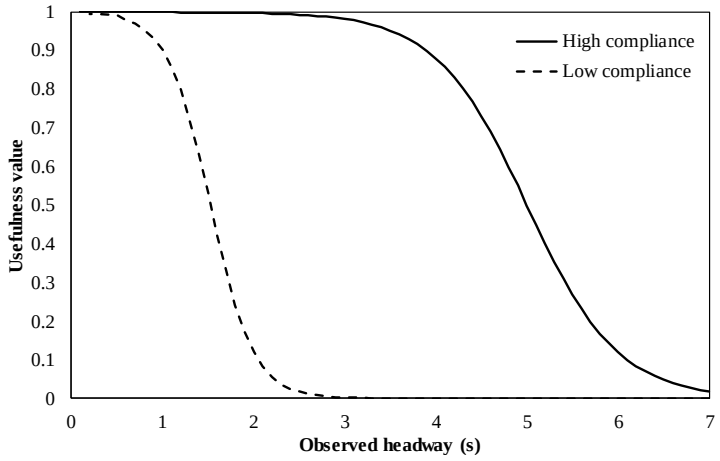

Figure 1 Difference between usefulness value function curves of high compliance ($\lambda = 10, \alpha = 0.65$) and low compliance levels ($\lambda = 6, \alpha = 0.65$).

3. INDICATORS OF TRAFFIC FLOW EFFICIENCY, AND SAFETY

3.1 Traffic disturbance indicators

This study analyses traffic flow disturbance in terms of traffic oscillation measures such as oscillation duration and oscillation amplitude. These measures are calculated when a traffic instability is induced via vehicles' braking hard manoeuvre on a single lane facility. This study adopts wavelet energy based method, as detailed in Zheng et al. (2011), to calculate oscillation duration and oscillation amplitude.

3.1.1 Traffic oscillation measures

The temporal distribution of wavelet-based energy E_b can assist in identifying significant changes in the time series of speed (Sharma et al., 2019c; Zheng et al., 2011; Zheng et al., 2013). A sharp increase in the wavelet energy distribution (Figure 2(b)) is witnessed corresponding to an abrupt change in the time series of speed (Figure 2(a)). The mathematical formulation of E_b is provided in Equation (9):

$$E_b = \frac{1}{max(a)} \int_0^{\infty} |T(a,b)|^2 \tag{9}$$

where $T(a,b)$ is a wavelet coefficient of a continuous signal and calculated as per Equation (10):

$$T(a,b) = \frac{1}{\sqrt{a}} \int_{-\infty}^{\infty} S(t) \psi \frac{t-b}{a} dt \tag{10}$$

where $S(t)$ is a continuous signal (time series of speeds in this case), $\psi \frac{t-b}{a}$ is a wavelet function, and a and b are scale and translation parameters of the wavelet function, respectively.

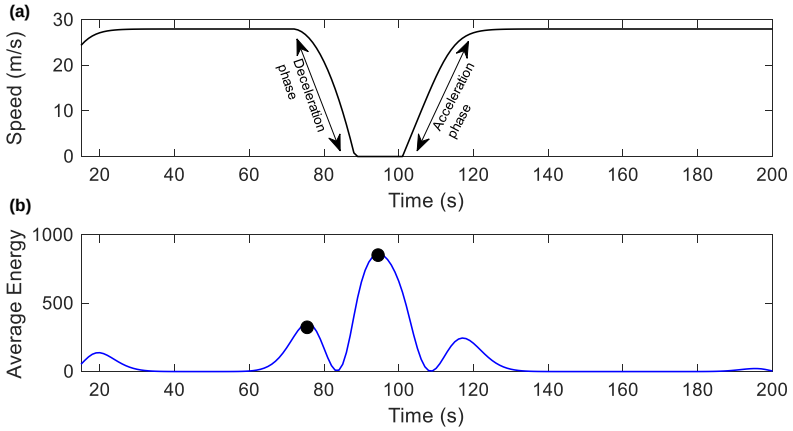

Figure 2 Illustrations of traffic oscillation and its detection using wavelet-based energy. (a) Time series of speed; (b) Wavelet based energy across scales (1 to 8) with change points identified.

There are hundreds of wavelets available in the literature and a few widely used wavelets are Haar, Daubechies family, Mexican hat, Morlet, and Coieflets family. Zheng and Washington (2012) presents a comprehensive examination of different wavelets' suitability in analysing traffic engineering related research topics, and concluded that the Mexican hat wavelet provides satisfactory performance in detecting traffic state change points, the start and the end of lane change manoeuvres, start points of acceleration (deceleration) waves, and discontinuity of the fundamental diagram. This study also employs the Mexican hat wavelet.

Oscillation duration (s): It is the duration of the deceleration phase measured as the time difference between when the first peak appears and when the second peak appears in the wavelet based energy curve. It is calculated for each vehicle in the platoon.

Average oscillation duration (s): This is calculated as $\frac{\sum_{i=1}^{i=k} OD_i}{k}$, where OD_i is the oscillation duration of the i^{th} vehicle in the platoon and k represents the last vehicle in the platoon. Note that vehicles in the platoon are numbered from 1 to k (the total number of vehicles in the platoon) moving from the head to the tail of the platoon.

Oscillation amplitude (m/s): It is calculated as the speed difference between the beginning (when the first peak appears) and the end of the deceleration phase (when the second peak appears).

Average oscillation amplitude (m/s): This is calculated as $\frac{\sum_{i=1}^{i=k} OA_i}{k}$, where OA_i is the oscillation amplitude of the i^{th} vehicle in the platoon and k represents the last vehicle in the platoon.

3.2 Traffic safety measures

Two surrogate measures of safety are employed in this study namely, modified time to collision (MTTC) and deceleration rate to avoid the crash (DRAC). Both MTTC and DRAC are widely used in the road safety literature (e.g., (Zheng et al., 2019; Zheng and Sayed, 2019)), and are discussed below.

3.2.1 Modified time to collision (MTTC)

The indicator $MTTC$ considers trajectory parameters such as relative distance, relative speed, and relative acceleration and calculates the time a following vehicle would take to collide with a lead vehicle if the vehicles do not change their movement characteristics (Ozbay et al., 2008). Equation (11) provides the mathematical formulation of $MTTC$.

$$MTTC = \frac{\Delta V_n \pm \sqrt{{\Delta V_n}^2 + 2\Delta a_n S_n}}{\Delta a_n} \tag{11}$$

Where ΔV_n is the relative speed (difference of the follower's speed V_n and the leader's speed (V_{n-1}))(m/s), S_n is the space gap (m), and Δa_n is the relative acceleration (difference of the follower's acceleration a_n and the leader's acceleration (a_{n-1}))(m/S^2). The final $MTTC$ is given by (i) if both of the $MTTC$ terms are positive, the minimum of them is considered to be the $MTTC$ value; and (ii) if one is positive while the other is negative, the positive outcome is considered to be the $MTTC$ value. Generally, a $MTTC$ below 1.5 s is considered unsafe.

3.2.2 Deceleration rate to avoid the crash (DRAC)

This study employs another safety measure, i.e., $DRAC$ and it is defined as the ratio of the square of the relative speed over the space gap as shown in Equation (12) (Almqvist et al., 1991). The American Association of State Highway and Transportation Officials recommends a deceleration rate of above 3.4 m/s^2 as unsafe.

$$DRAC = \frac{(\Delta V_n)^2}{S_n} \tag{12}$$

When presenting results in Section 5, the notations $MTTC$ and $DRAC$ are used to indicate $MTTC$ and $DRAC$ at vehicle level, respectively, and minimum $MTTC$ and minimum $DRAC$ are used are used to indicate $MTTC$ and $DRAC$ at platoon level, respectively. These are defined in Equations (13), (14), (15), and (16).

$$MTTC = \min(MTTC_1, MTTC_2, \dots, MTTC_i, \dots, MTTC_n) \tag{13}$$

$$DRAC = \min(DRAC_1, DRAC_2, \dots, DRAC_i, \dots, DRAC_n) \tag{14}$$

$$minimum\ MTTC = \min(MTTC^1, MTTC^2, \dots, MTTC^j, \dots, MTTC^k) \tag{15}$$

$$minimum\ DRAC = \min(DRAC^1, DRAC^2, \dots, DRAC^j, \dots, DRAC^k) \tag{16}$$

where $MTTC_i$ is calculated using Equation (11) and i represents a time instant between the start of a follower's trajectory ($t = 1$) and the end of the follower's trajectory ($t = n$). $DRAC_i$ is

calculated using Equation (12). $MTTC^j$ is calculated using Equation (13) for the j^{th} follower, and j varies from *2* to *k*. Moreover, $DRAC^j$ is calculated using Equation (14).

3.3 Traffic efficiency indicators

Fundamental traffic flow parameters are utilised as indicators of traffic efficiency. The average flow (mentioned by the reviewer) and average speed have been used as indicators of traffic efficiency in previous studies as well (Brilon et al., 2005; Friedrich, 2016). The estimation of these parameters is detailed in the next section.

3.3.1 Estimation of fundamental parameters of traffic flow

There are three methods to estimate the fundamental traffic flow parameters i.e., flow (q), density (k), speed (V), namely the highway capacity manual (HCM) method, the x-t method based on Edie's generalised definition (Edie, 1963), and the n-t method. The HCM method is based on the well-known definitions of flow, density, and speed, and the fundamental relationship between these three flow parameters. The x-t method estimates flow, density, and speed using the trajectory data, whereas the n-t method is based on the cumulative number of vehicles in the cumulative number-time (n-t) domain. The x-t method is preferred in this study since this study utilises trajectory data. The method is described in the paragraphs below. Refer to Ni and Leonard (2006) for a description of the HCM method and the n-t method.

Edie's generalised definitions are applied to calculate flow (q), density (k), speed (V) when trajectory data are available (Edie, 1963). According to Edie, the flow is given by the total distance travelled by all vehicles in area A divided by the area of A, i.e., $|A|$ as shown in Equation (17). The density is given by the total time spent by all vehicles in A divided by $|A|$ as shown in Equation (18). Finally, the speed is calculated as per the fundamental relationship, i.e., flow over density and in terms of Edie's definition as the ratio of the total distance travelled by all vehicles in A over the total time spent by in A as shown in Equation (19).

$$q = \frac{d(A)}{|A|} \tag{17}$$

$$k = \frac{t(A)}{|A|} \tag{18}$$

$$V = \frac{d(A)}{t(A)} = \frac{q}{k} \tag{19}$$

where $d(A)$ is the total distance travelled by all vehicles in A and $t(A)$ is the total time spent by all vehicles in A. The quantities $d(A)$, $t(A)$, and $|A|$ are provided in Equations (20), (21), and (22).

$$d(A) = \sum_{i=1}^{n} \{\min\left(x^{(i)}(t_u), x_u\right) - \max(x^{(i)}(t_l), x_l)\} \tag{20}$$

$$t(A) = \sum_{i=1}^{n} \{\min\left(t^{(i)}(x_u), t_u\right) - \max(t^{(i)}(x_l), t_l)\} \tag{21}$$

$$|A| = (x_u - x_l) \times (t_u - t_l) \quad (22)$$

where n is the total number of trajectories in A, x_l and x_u are the lower and the upper bounds of A in x domain, respectively, t_l and t_u are the lower and the upper bounds of A in t domain, respectively, $x^{(i)}(t_l)$ and $x^{(i)}(t_u)$ are the locations of the i^{th} vehicle at time t_l and t_u, respectively, and $t^{(i)}(x_l)$ and $t^{(i)}(x_u)$ are the time values when the i^{th} vehicle passes locations x_l and x_u, respectively. Figure 3 illustrates the Edie's method. Note that average density values are calculated but not reported in this study. Traffic measurement devices, such as loop detectors installed beneath the road surface, can be used to measure flows, densities and average vehicle velocities in ways that are consistent with these generalised definitions. A detailed discussion on this can be found in (Cassidy and Coifman, 1997).

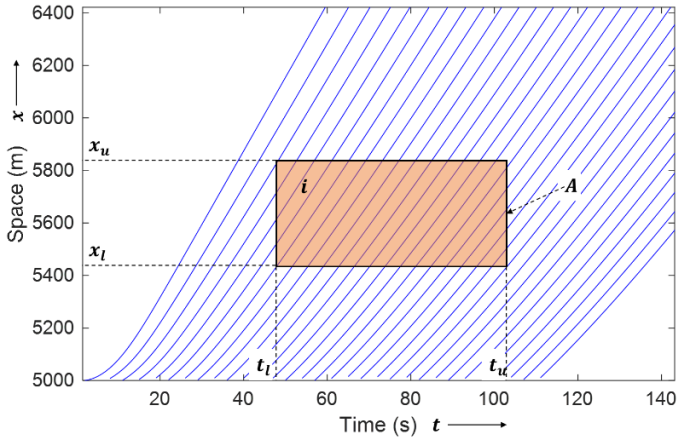

Figure 3 The *x-t* method based on Edie's generalised definition

4. MIXED TRAFFIC SCENARIOS AND EXPERIMENTS DESIGN

4.1 General

In this study, a connected environment is simulated in which vehicles are communicating with surrounding vehicles via vehicle-to-vehicle communication. It is assumed that vehicles are fitted with the onboard driver assistance system devices that are displaying information on the wind screen (similar to the heads-up display). The primary motivation behind such a simulation design is the previous advanced driving simulator based connected environment studies (Sharma et al., 2020, 2019b). In the experiment, the connected environment was cautiously designed after a comprehensive review of the literature on in-vehicle driver assistance systems and the current driving aids provided by major car manufacturers. The full information on how the driving simulator experiment was designed can be found in (Ali et al., 2020). We have assumed the continuous information (the information is always present on the windscreen) is available to drivers in the simulation. The continuous information includes messages about the speed of and the spacing to the leader. As per Sharma et al. (2019c), when continuous information is provided, drivers maintain larger time gaps (thereby safety gaps as well) and there are fewer fluctuations in speed and spacing as compared to when no information is provided. The degree of increase in the time-gap or decrease in fluctuations depends on the degree of driver compliance with the information. CVDS-IDM utilised in this study to simulate

the car-following behaviour can capture these changes in driving behaviour due to the continuous information and degree of compliance with the information. A rigorous assessment on the performance of CVDS-IDM can be found in Sharma et al. (2019b). As such, high compliance and low compliance drivers are also simulated. Note that for readers who are interested in car following model (IDM in particular) calibration, refer to Punzo et al. (2015), Ciuffo et al. (2013); da Rocha et al. (2015) and Sharmar et al. (2019a).

Two experiments namely, Experiment 1 and Experiment 2 are performed where the former is used to measure traffic flow disturbance, efficiency, and safety while the latter is used to measure traffic flow fundamental parameters. Experiment 1 mimics a scenario where the platoon leader stops for a short period and then starts accelerating causing a backward propagating wave, whereas Experiment 2 mimics a heavily congested scenario generated by stopping the platoon leader more than once and for a long period (mimicking a sluggish leader), e.g., the magnitudes of oscillation duration and amplitude will be high in Experiment 2. Note that these two separate experiments are performed for the ease of visualising, understanding, and discerning the benefits of CVs. Moreover, in both the experiments, a single lane facility is assumed to avoid lane changes.

Each experiment has seven scenarios characterised by seven different mixed traffic environments including All TVs (consisting of only TVs), All CV-LCs (consisting of CVs with low compliance drivers), All CV-HCs (consisting of CVs with high compliance drivers), TV and CV-LC (consisting a mix of TVs and CVs with low compliance drivers), TV and CV-HC (consisting a mix of TVs and CVs with high compliance drivers), CV-LC and CV-HC (consisting a mix of CVs with high compliance and low compliance drivers), and TV, CV-LC and CV-HC (consisting a mix of TVs, CVs with low compliance drivers, and CVs with high compliance drivers). Here, LC and HC represent low compliance and high compliance drivers, respectively. The penetration rate of CVs varies from 0% to 100% in mixed traffic environments of TV and CV-LC, and TV and CV-HC and the penetration rate of CV-HC varies from 0% to 100% in the case of mixed traffic of CV-LC and CV-HC. Furthermore, the penetration rate of CV-LC and CV-HC is fixed to 33 % each when generating the mixed traffic of TV, CV-LC, and CV-HC to avoid any repetition of previously generated scenarios. Table 1 summarizes all the mixed traffic scenarios and experiments considered in this study.

4.2 A description of the three platoon policies: the best and the worst spatial arrangements

As discussed in the introduction section, the spatial arrangement of CVs in a platoon plays a major role in achieving the maximum benefits from CVs at a given penetration rate. In this regard, this study considers three platoon policies characterised by different spatial arrangements. The first platoon policy is termed as the best case that results in the maximum benefit from CVs. The second platoon policy is termed as the worst case that results in the minimum benefit from the CVs at a given penetration rate. The third platoon policy is termed as the random case that results in the random arrangement of the CVs in the mixed traffic and the benefits are expected to fall within the best and the worst spatial arrangement. The arrangement of CVs in the best and the worst case is described in the next paragraph.

For example, consider a mixed traffic platoon of TVs and CV-HCs of 31 vehicles with 50% penetration of CV-HCs (i.e., 15 vehicles). Importantly, for a single lane facility, there can be four combinations of car-following interactions in the platoon including (1) a TV following a TV, (2) a CV following a CV, (3) a CV following a TV, and (4) a TV following a CV. A CV will behave like a CV only when it is following another CV; otherwise, it will behave like TV since it will not receive any information from the front vehicle. Moreover, as conjectured in previous studies, CVs have the potential to more efficiently bear and suppress the negative impact of backward propagating waves as compared to TVs. Hence, the best arrangement will correspond to a situation when all 15 CVs in the platoon are grouped together and placed at the front of the platoon whereas the worst arrangement will correspond to a situation when all 15 CVs are distributed such that one CV is placed between two TVs resulting in CVs behaving like TVs.

Table 1 A description of the design of the experiments in this study.

Experiment	Traffic composition	Scenarios	Penetration rate of CVs	Platoon policies	Leader's speed profile	Measures calculated
Experiment 1	Homogenous	All TVs	0%	-	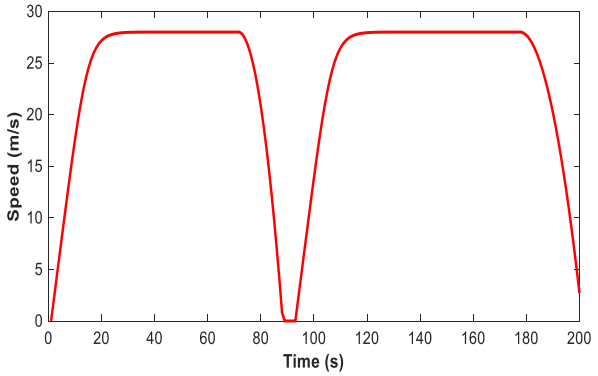	**Traffic flow disturbance:** Oscillation duration, Oscillation amplitude; **Traffic Safety:** MTTC, and DRAC
		All CV-HCs	100%			
		All CV-LCs	100%			
	Heterogenous	TVs and CV-HCs	0-100%	1) Best spatial arrangement 2) Worst spatial arrangement 3) Random arrangement		
		TVs and CV-LCs	0-100%			
		CV-HCs and CV-LCs	0-100%			
		TVs and CV-HCs and CV-LCs	33% each			
Experiment 2	Homogenous	All TVs	0%	-	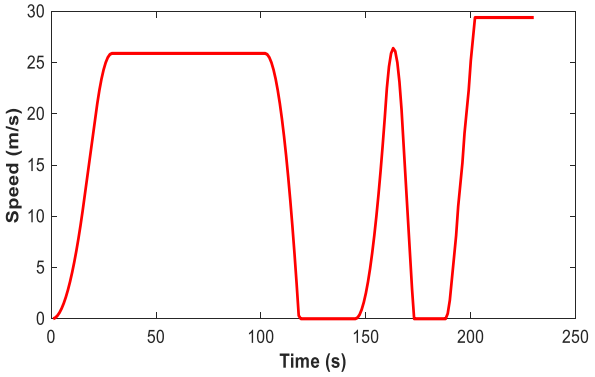	**Traffic Efficiency:** Average flow and Average speed
		All CV-HCs	100%			
		All CV-LCs	100%			
	Heterogenous	TVs and CV-HCs	0-100%	1) Best spatial arrangement 2) Worst spatial arrangement 3) Random arrangement		
		TVs and CV-LCs	0-100%			
		CV-HCs and CV-LCs	0-100%			
		TVs and CV-HCs and CV-LCs	33% each			

Figure 4 compares the best arrangement with the worst at 50% penetration rate of CVs. It depicts that wave propagation diminishes early in the case of the best arrangement compared to the worst arrangement. Table 1 details how the best, the worst, and the random spatial arrangement is achieved in each mixed traffic scenario.

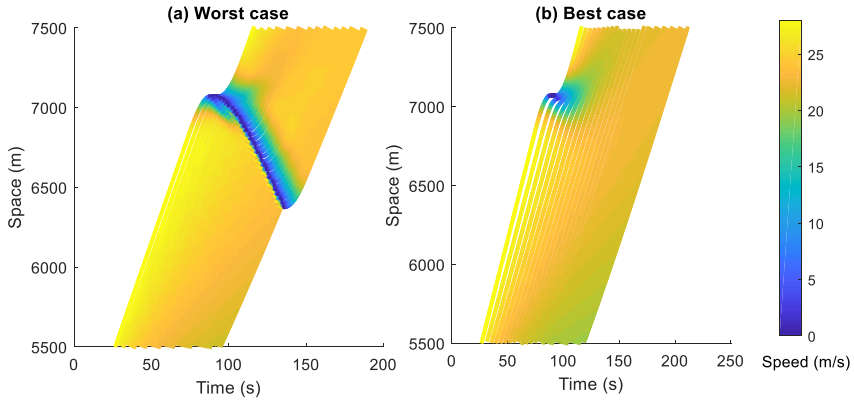

Figure 4 A comparison of the worst spatial arrangement and the best spatial arrangement of CVs.

Table 2 A description of the best, the worst, and the random spatial arrangements definitions corresponding to the mixed traffic environments.

Mixed traffic Environment	**Platoon policy 1: the best spatial arrangement**	**Platoon policy 2: the worst spatial arrangement**	**Platoon policy 3: the random spatial arrangement**	**Conditions**
All TVs All CV-LCs All CV-HCs	Not applicable since no mixed traffic			
TVs and CV-LCs	CVs are placed at the front of the platoon	Each CV is placed between two TVs in the platoon	CVs (CV-HCs or CV-LCs) are arranged randomly in the mixed traffic	If the penetration rate is 50% or less
TVs and CV-HCs		First CVs equal to the number of TVs are arranged such that each CV is placed between two TVs in the platoon and then rest of the CVs are placed at the end of the platoon		If the penetration rate is more than 50%

CV-LCs and CV-HCs	CV-HCs are placed at the front of the platoon	CV-HCs are placed at the end of the platoon	CV-HCs are arranged randomly in the mixed traffic
TVs, CV-LCs, and CV-HCs	CV-LCs follow CV-HCs and these are followed by TVs	Each CV-HCs is placed between two TVs in the platoon and CV-LCs are placed at the end	CVs (CV-HCs or CV-LCs) are arranged randomly in the mixed traffic

One may question the importance of simulating the worst case scenario since we already know that the distribution of CV is worst case. The simulation of the worst case scenario answers the following questions how bad could the worst case scenario be? What is the disparity between the best case and the worst case scenario results? Is this disparity acceptable? How do the worst case and the best case pan out for the mixed traffic of CV-HCs and CV-LCs? On the conceptual and qualitative basis, answering the stated questions will be less comprehendible, and provide limited value in operating and controlling mixed traffic. Moreover, the worst case scenario becomes even more important since the best case, the worst case, and the random case cover the whole spectrum and provide a complete understanding of the characteristics of mixed traffic of CVs and TVs.

Note that in the case of random arrangement, each scenario is simulated 100 times, and the average values of all metrics and parameters are reported for each scenario.

4.3 Design of Experiment 1

The aim of Experiment 1 is to investigate traffic flow efficiency, and safety of the mixed traffic stream when the platoon leader undergoes one stop and go cycle. To this end, a platoon of 31 vehicles is generated on a single-lane facility of 5 km. The first vehicle's trajectory is generated manually. At $t = 1$ s, the leader is $5000\,m$ ahead of the reference point (the leader's position $x_{n-1}(1) = 15000\,m$, speed $v_{n-1}(1) = 0\,m/s$, and acceleration $\mathrm{a}_{\mathrm{n-1}}(1) = 0\ \mathrm{m/s^2}$). At $t = 1.1$ s the leader starts accelerating and attains a speed v_{n-1} of 28 m/s at $t = 30$ s and maintain it until $t = 72$ s. From $t = 72.1$ s, the leader starts decelerating and stops at $t = 89$ s. The leader starts accelerating at $t = 101$ s, attains the speed $v_{n-1} = 28$ m/s at $t = 130$ s, and maintains it until the end of the experiment, i.e., $\mathrm{t} = 200$ s. Refer to Table 1 for the leader's speed profile.

Table 3 Car-following models parameters assumed for simulation in the experiments.

Experiment 1 and 2			
Parameters	**HIDM**	**CVDS-IDM (LC)**	**CVDS-IDM (HC)**
$V_0\ (m/s)$	29	29	29
δ	4	4	4
$T\ (s)$	1.5	1.5	1.5
s_0 (m)	5	5	5
$a\ (\mathrm{m/s^2})$	2.5	2.5	2.5
$b\ (\mathrm{m/s^2})$	2.5	2.5	2.5
σ_r	0.05	-	-
V_s	0.01	-	-
$\tilde{\tau}\ (s)$	20	-	-
α	-	0.7	0.2
γ	-	0.65	0.65
λ	-	6	10

The rest of the 30 vehicles' trajectories are simulated using car-following models. For HIDM drivers, CVDS-IDM low compliance drivers, and CVDS-IDM high compliance drivers, the parameters are set as provided in Table 3. The parameters for CVDS-IDM low compliance and CVDS-IDM high compliance are set based on the calibration results from our previous study (Sharma et al. (2019b)) and they can successfully capture low and high compliance properties e.g., observe Figure 1 and its explanation in Section 2.2.1. Figure 5 displays the platoons of All TVs, All CV-LCs, and All CV-HCs traffic environments resulting from Experiment 1. The figure depicts that, keeping other confounding factors the same, oscillations propagate towards the end of the platoon in the case of All TVs whereas it diminishes significantly before reaching the end of the platoon in the cases of All CV-LCs and All CV-HCs. Furthermore, the platoon of All CV-HCs is more efficient (oscillations dampen early) relative to All CV-LCs.

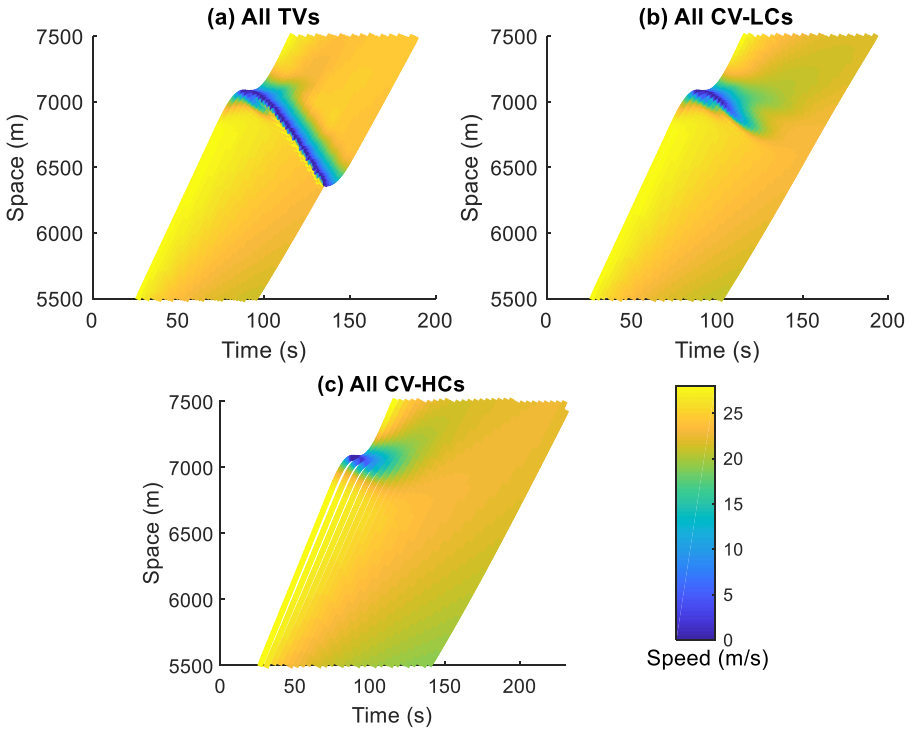

Figure 5 Examples of platoons generated in Experiment 1. (a) All TVs case; (b) All CV-LCs case; and (c) All CV-HCs case.

4.4 Design of Experiment 2

The purpose of Experiment 2 is to estimate the fundamental traffic flow parameters in a heavily congested traffic environment. To this end, a platoon of 61 vehicles is generated on a single-lane facility of 5 km. The first vehicle's trajectory is generated manually. At $t = 1$ s, the leader is 15000 m ahead of the reference point (the leader's position $x_{n-1}(1) = 15000$ m, speed $v_{n-1}(1) = 0$ m/s, and acceleration $a_{n-1}(1) = 0$ m/s^2). At t $= 1.1$ s the leader starts accelerating, attains a speed v_{n-1} of 25.9 m/s at t $= 30$ s, and maintains it until t $= 100$ s. A traffic signal is positioned 270 m ahead of this point. From $t = 100.1$ s, the leader starts decelerating and stops at $t = 119$ s. The leader starts accelerating at $t = 146$ s, attains a speed v_{n-1} of 26 m/s at $t = 162$ s. After this, the leader starts decelerating again at $t = 164$ s and stops at $t = 173$ s. After 15 s, the leader starts accelerating again, attains $v_{n-1} = 29\ m/s$ at $t = 202$ s, and maintains until the end of the experiment, i.e., $t = 230$ s. Refer to Table 1 for the leader's speed profile.

Same as Experiment 1, the rest of the 60 vehicles' trajectories are simulated using car-following models. For HIDM drivers, CVDS-IDM low compliance drivers, and CVDS-IDM high compliance drivers, the parameters are set as provided in Table 3. Figure 6 displays the platoons of All TVs, All CV-LCs, and All CV-HCs traffic environments resulting from Experiment 2. The figure reveals that keeping other confounding factors same, heavy congestion builds up in the case of All TVs whereas the congestion clears significantly before reaching the end of the platoon in the case of All CV-HCs. Furthermore, the platoon of All CV-LCs does display the propagation of congestion to the end of the platoon even though the impact is less severe than

the case of All TVs. In addition, station locations between 16000 m and 18000 m record heavy congestion in Experiment 2 in the case of All TVs. This study focusses on average flow and average speed values calculated at stations placed between 16000 m and 18000 m.

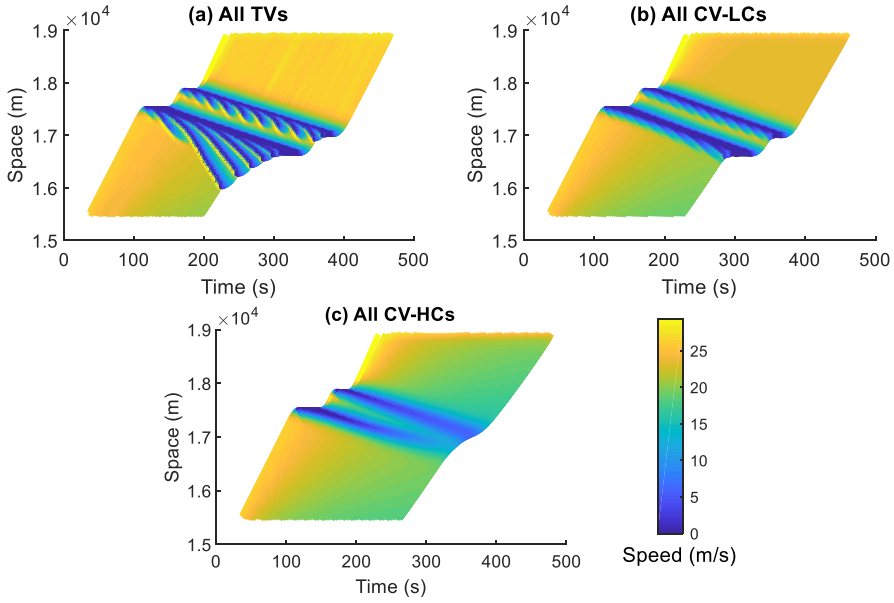

Figure 6 Examples of platoons generated using Experiment 2. (a) All TVs case; (b) All CV-LCs case; and (c) All CV-HCs case.

5. RESULTS AND DISCUSSIONS

5.1 Experiment 1 Results

5.1.1 Homogenous traffic scenarios: All TVs, All CV-LCs, and All CV-HCs

Figure 7 displays traffic flow efficiency, and safety measures computed for all the three scenarios: All TVs, All CV-LCs, and All CV-HCs. The figure reveals that moving from the head to the tail of the platoon both the amplitude and the duration decrease to 0 for All CV-LCs and All CV-HCs. Moreover, the oscillations dampen quickly for All CV-HCs as compared to All CV-LCs. Conversely, for All TVs, when moving backward from the head of the platoon the amplitude and the duration decrease to 20 m/s and 10 s, respectively, and then remains fairly constant till the end of the platoon. The MTTC value increases to 10 s for both All CV-LCs and All CV-HCs when moving from the head to the tail of the platoon whereas, for All TVs case, the majority of MTTC values are in the range of 1.5 to 2 s throughout the platoon. The DRAC values quickly decrease to 0 m/s^2 when moving from the head of the platoon in the case of All CV-HCs, and moderately increases and then decreases in the case of All CV-LCs. However, an overall increasing trend has been witnessed for a platoon of All TVs.

The above results underscore benefits of CVs over TVs. More specifically, when drivers receive surrounding traffic information they make better decisions thereby reducing traffic flow disturbance, and enhancing safety. The results also demonstrate that the high compliance drivers drive more efficiently and are at a lower risk than low compliance drivers.

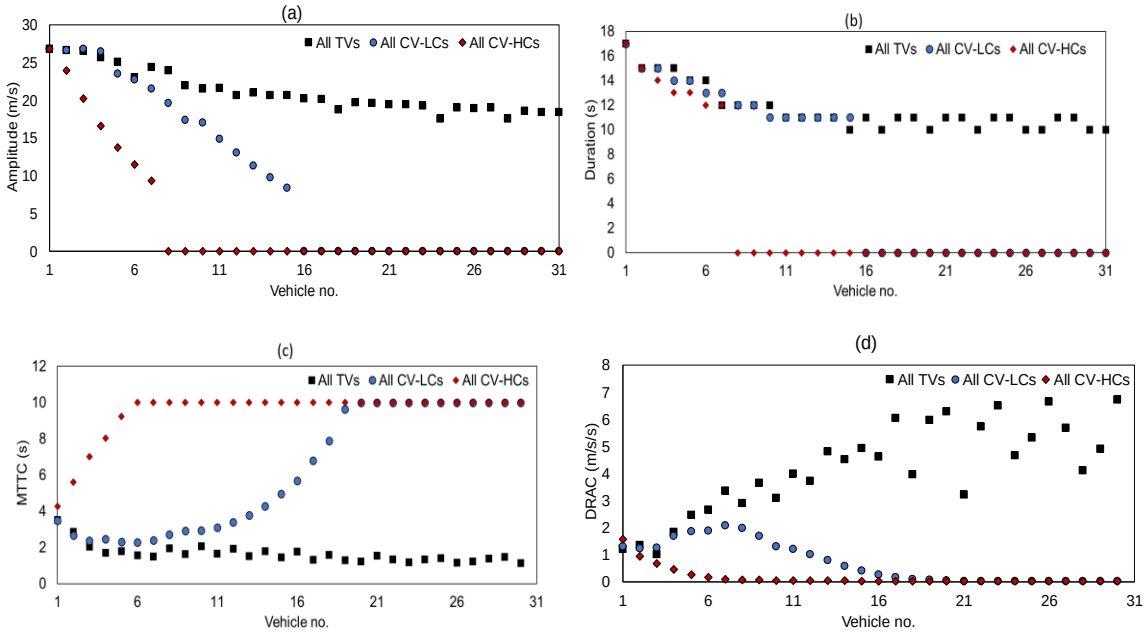

Figure 7 Measures of traffic flow efficiency, and safety for All TVs, All CV-LCs, and All CV-HCs. (a) Oscillation amplitude; (b) Oscillation duration; (c) MTTC; and (d) DRAC.

5.1.2 Mixed traffic scenarios: TVs and CV-LCs, and TVs and CV-HCs

Figures 8 and 9 illustrate the importance of the spatial arrangement of CVs in a mixed platoon of TVs and CVs at different penetration rates of CVs. If CVs are arranged in the best spatial arrangement, a low average oscillation amplitude, a low average oscillation duration, a high minimum MTTC, and a low maximum DRAC are witnessed as the penetration rate of CVs (CV-LCs or CV-HCs) increases in the mixed platoon. Moreover, the benefits can be observed even at low penetration rates such as 10%, 30%, and 40% if CVs are arranged according to the best spatial arrangement. On the contrary, a high average oscillation amplitude, a high average oscillation duration, a low minimum MTTC, and a high maximum DRAC can be observed even at a penetration rate as high as 80% if CVs are arranged in the worst spatial arrangement. In the best spatial arrangement case, it is remarkable that the benefits achieved at 100% penetration rate of CVs are equivalent to the benefits achieved with only 10% penetration rate of CVs.

In the case of random arrangement, as the penetration rate increases, average amplitude, average duration, and maximum DRAC decreases while minimum MTTC increases. Data points corresponding to the random arrangement lies between the best and the worst arrangements as expected.

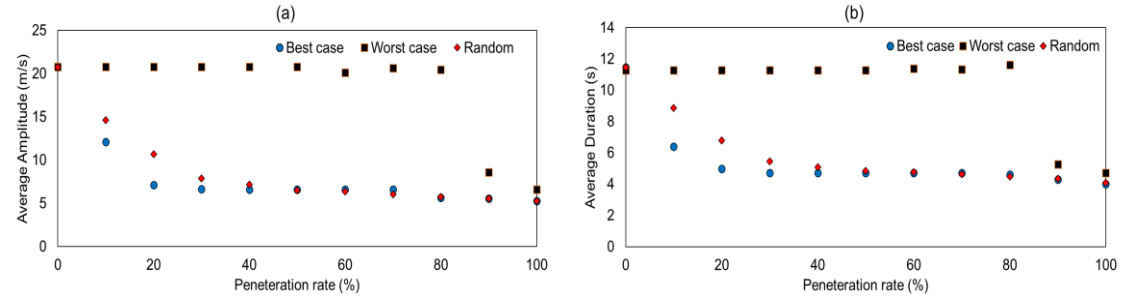

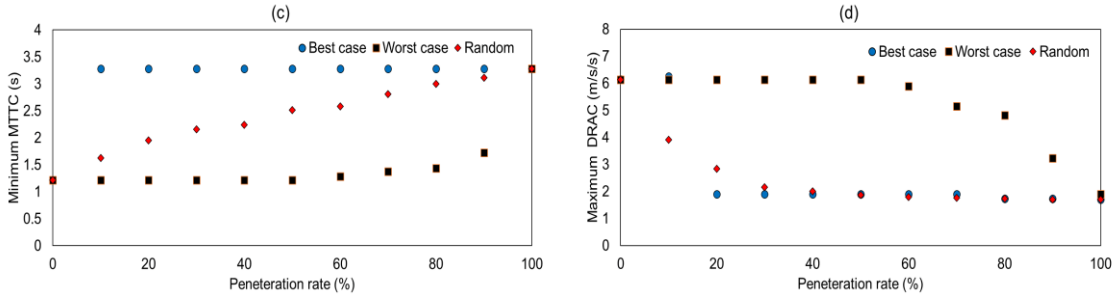

Figure 8 A comparison of measures of the traffic flow disturbance and safety among the best, the worst, and the random spatial arrangements of CVs at different penetration rates – Scenario TVs and CV-LCs. (a) Average oscillation amplitude; (b) Average oscillation duration; (c) Minimum MTTC; and (d) Maximum DRAC.

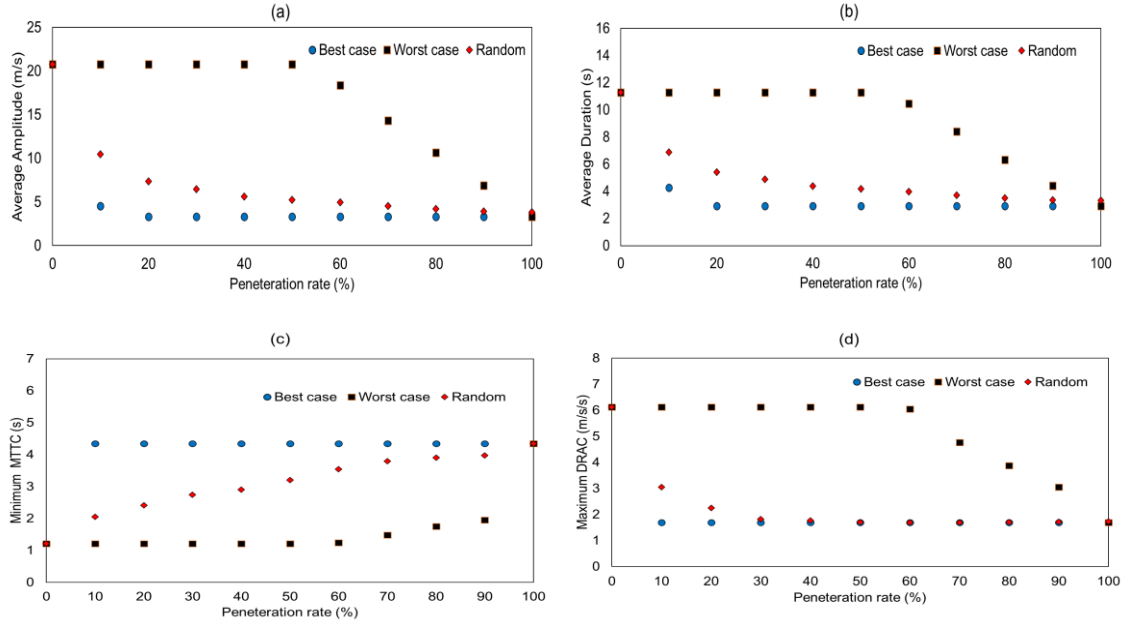

Figure 9 A comparison of measures of the traffic flow disturbance and safety among the best, the worst, and the random spatial arrangements of CVs at different penetration rates – Scenario TVs and CV-HCs. a) Average oscillation amplitude; (b) Average oscillation duration; (c) Minimum MTTC; and (d) Maximum DRAC.

5.1.3 Mixed traffic scenario of CV-LCs and CV-HCs

Figure 10 illustrates the impact of the spatial arrangement of vehicles on traffic flow efficiency, and safety of the mixed traffic flow of CV-LCs and CV-HCs. In this case, the penetration rate of CV-HCs ranges from 0% to 100%. The figure reveals that overall, average oscillation amplitude, average oscillation duration, minimum MTTC, and maximum DRAC are acceptable at all penetration rates since the platoon consists of CVs only. However, the best spatial arrangement of CV-HCs can further reduce traffic flow disturbances and increase safety at a penetration rate as low as 10%. Conversely, the worst spatial arrangement of CV-HCs can result in relatively high traffic flow disturbances and low safety at a penetration rate as high as 80%. Moreover, in the case of random arrangement, as the penetration rate of CV-HCs

increases, average oscillation amplitude, average oscillation duration, maximum DRAC decreases and minimum MTTC increases.

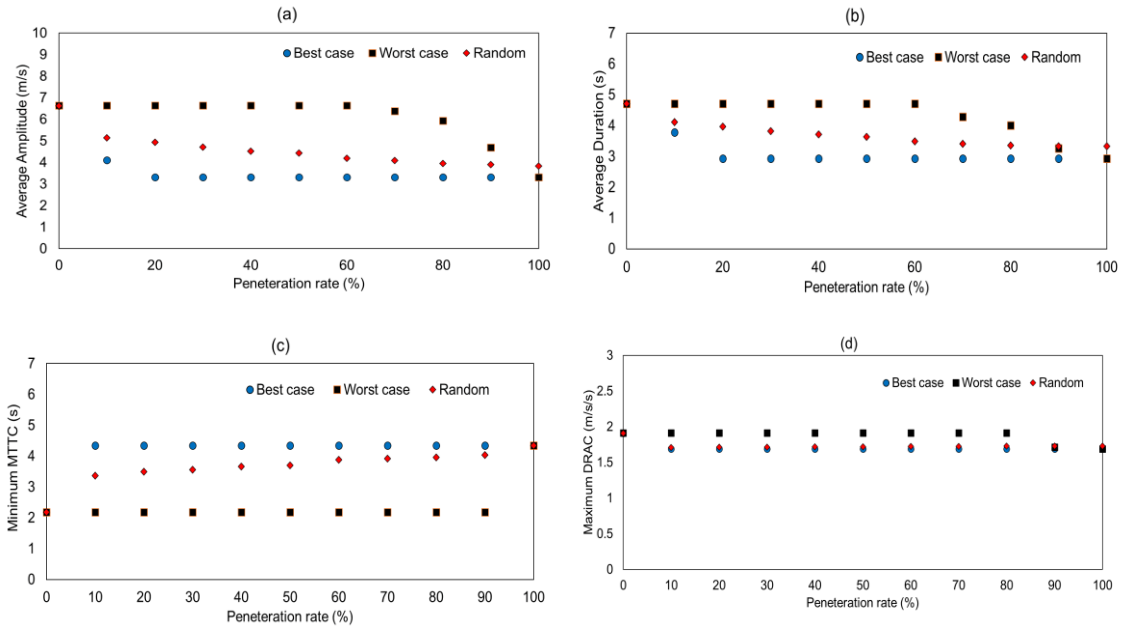

Figure 10 A comparison of measures of the traffic flow disturbance and safety among the best, the worst, and the random spatial arrangements of CVs at different penetration rates of CV-HCs – Scenario CV-HCs and CV-LCs. a) Average oscillation amplitude; (b) Average oscillation duration; (c) Minimum MTTC; and (d) Maximum DRAC.

5.1.4 Mixed traffic scenario of TVs, CV-LCs and CV-HCs

Figure 11 illustrates the impact of the best and the worst spatial arrangements on the mixed traffic of TVs, CV-LCs, and CV-HCs. As discussed previously, traffic oscillations dampen early for the best spatial arrangement relative to the worst spatial arrangement. In addition, a high MTTC value and a low DRAC value are achieved early in the best case scenario as compared to the worst case scenario. In the case of random arrangement, the oscillation amplitude, oscillation duration, and maximum DRAC decreases whereas MTTC increases. Moreover, the figure reveals that MTTC value decreases and DRAC value increases towards the tail of the platoon in the best spatial arrangement case. This is because all TVs are placed at the end of the platoon. For the same reason, the random arrangement offers relatively high safety margin as compared to the best case towards the end of the platoon.

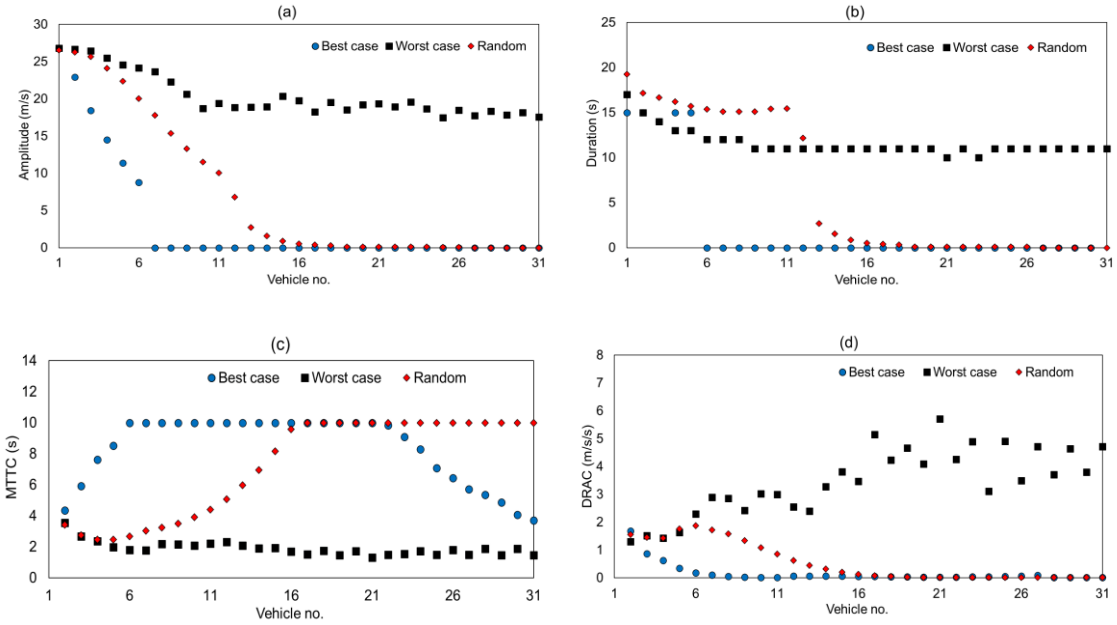

Figure 11 A comparison of measures of the traffic flow disturbance and safety among the best, the worst, and the random spatial arrangements of CVs of CVs at 33% penetration rate – Scenario TVs, CV-LCs, and CV-HCs. (a) Oscillation amplitude; (b) Oscillation duration; (c) MTTC; and (d) DRAC.

5.2 Experiment 2 Results

5.2.1 Homogenous traffic scenarios: All TVs, All CV-LCs, and All CV-HCs

Figure 12 displays the average flow and the average speed computed at each station location for all three scenarios. Note that the road section between 16000 m to 18000 m depicts the heavily congested section of the road considered in Experiment 2. As the figure reveals, in the heavily congested section, the flow rate is the highest in the case of All CV-HCs which is followed by All CV-LCs and the lowest flow rate is observed for All TVs case. Similarly, the highest and the lowest speeds are witnessed for All CV-HCs and All TVs, respectively. These results signify that a stream of CVs is more efficient as compared to TVs in the case of a sluggish leader. Under uncongested traffic conditions, the average flow and average speed are high for all TVs as compared to all CV-HCs and all CV-LCs. This is contrary to what has been reported in previous studies i.e., a platoon of CVs will always result in the high average flow and average speed. The reason behind this is the large time gap maintained by CV-HCs and CV-LCs as compared to all TVs.

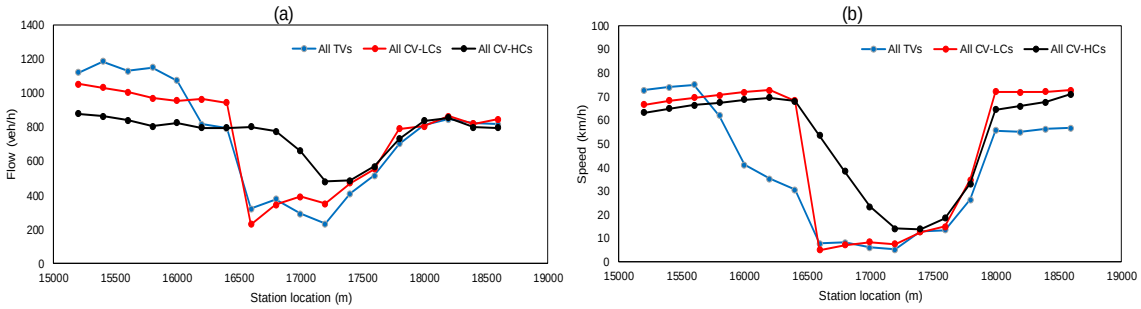

Figure 12 A comparison of fundamental traffic flow parameters among All TVs, All CV-LCs, and All CV-HCs. (a) Average flow; and (b) Average speed.

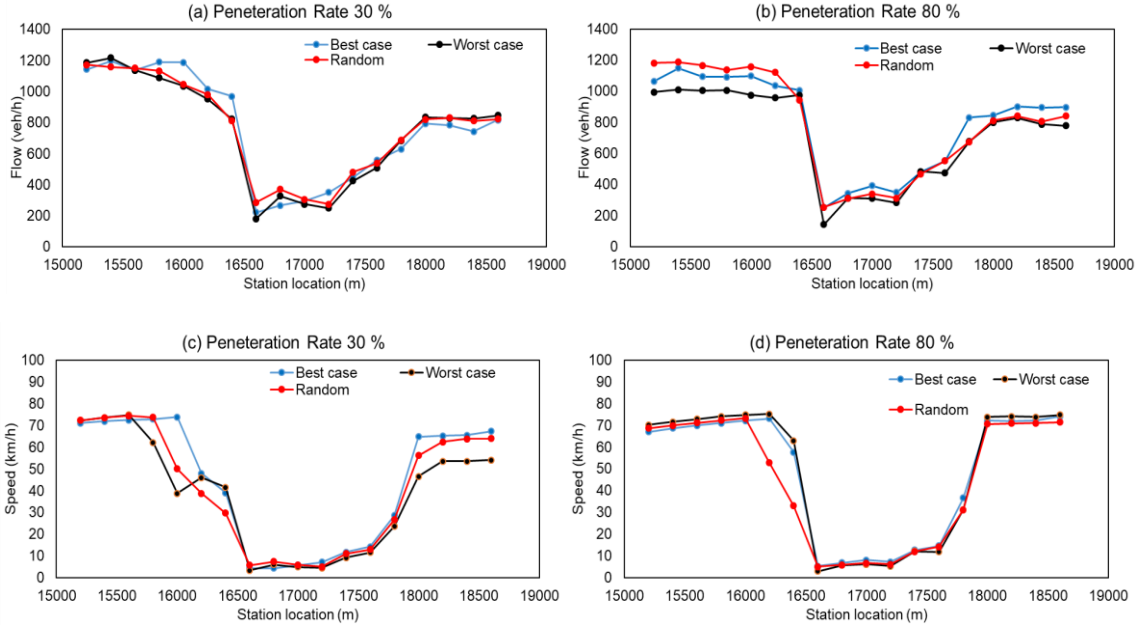

Figure 13 A comparison of fundamental traffic flow parameters among the best, the worst, and the random spatial arrangements at different penetration rates– Scenario TVs and CV-LCs. (a) Average flow at 30% penetration rate; (b) Average flow at 80% penetration rate; (c) Average speed at 30% penetration rate and (d) Average speed at 80% penetration rate.

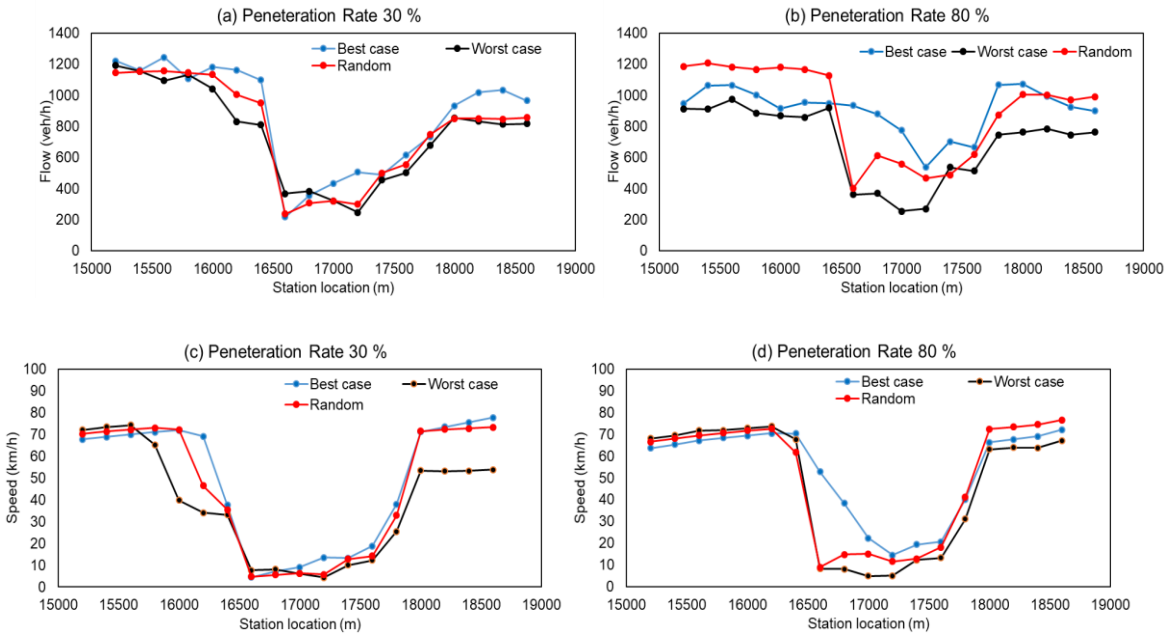

Figure 14 A comparison of fundamental traffic flow parameters among the best, the worst, and the random spatial arrangements at different penetration rates– Scenario TVs and CV-HCs. (a) Average flow at 30% penetration rate; (b) Average flow at 80% penetration rate; (c) Average speed at 30% penetration rate and (d) Average speed at 80% penetration rate.

5.2.2 Mixed traffic scenarios: TVs and CV-LCs, and TVs and CV-HCs

Figures 13 and 14 illustrate the importance of the spatial arrangement of CVs in a mixed platoon of TVs and CVs at different penetration rates of CVs. The benefits of CVs characterised by a higher flow and speed in the heavily congested section are witnessed as the penetration rate of CVs (CV-LCs or CV-HCs) increases in the mixed platoon and CVs are arranged in the best spatial arrangement. Moreover, the benefits can be observed even at low penetration rate such as 30% if CVs are arranged in the best spatial arrangement. Comparing Figures 13 and 14 imparts that the mixed traffic of TVs and CV-HCs is benefitted more (characterised by higher flow and speed values in the congested section) with the best spatial arrangement as compared to the mixed traffic of TVs and CV-LCs with the best spatial arrangement. These observations signify that the best spatial arrangement of high compliance drivers boosts the benefits of CVs relative to low compliance drivers. In the case of random arrangement, at 80% penetration rate, the average flow and average speed values are between the best case and the worst scenarios at the heavily congested section. This aspect is prominent for the TV and CV-HCs mixed traffic case.

5.2.3 Mixed traffic scenario of CV-LCs and CV-HCs

Figure 15 illustrates the impact of the spatial arrangement of vehicles on the average flow and the average speed of the mixed traffic flow of CV-HCs and CV-LCs. The figure reveals that in the congested section, overall, the average flow and the average speed values are higher as compared to those obtained in the previous mixed traffic scenarios. This is because the platoon consists of only CVs. The best spatial arrangement of CV-HCs can further increase the average flow and the average speed at a penetration rate as low as 30%. On the other hand, the worst

spatial arrangement of CV-HCs can decrease the average flow and the average speed at a penetration rate as high as 80%. In the case of random arrangement, at both 30% and 80% penetration rates, the average flow and average speed values are between the best case and the worst scenarios at the heavily congested section.

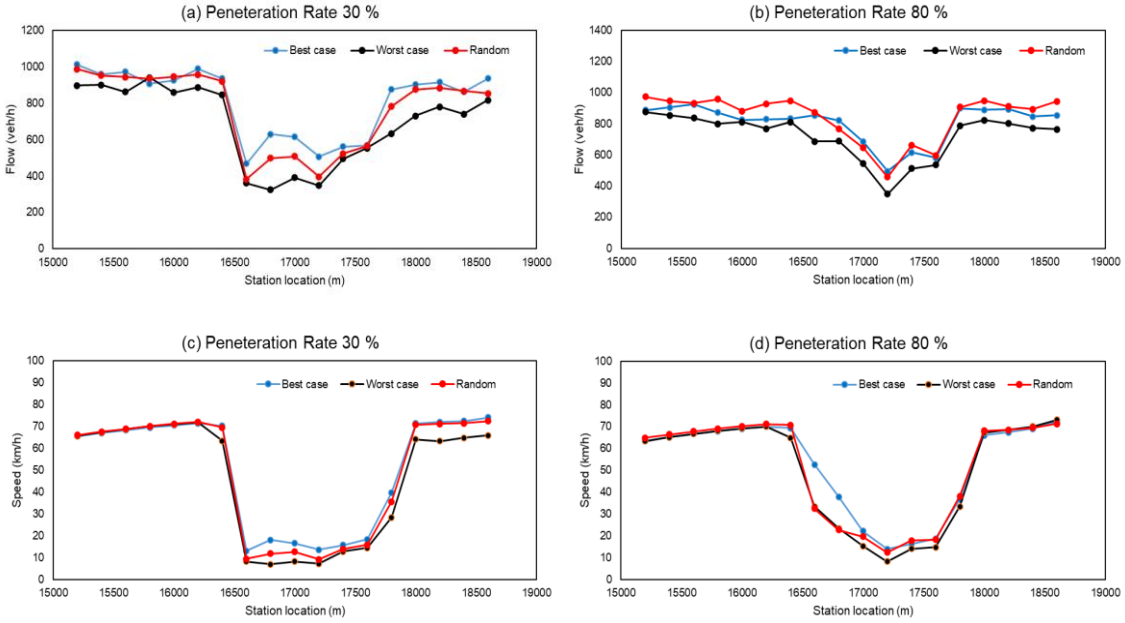

Figure 15 A comparison of fundamental traffic flow parameters among the best, the worst, and the random spatial arrangements at different penetration rates– Scenario CV-LCs and CV-HCs. (a) Average flow at 30% penetration rate; (b) Average flow at 80% penetration rate; (c) Average speed at 30% penetration rate and (d) Average speed at 80% penetration rate.

5.2.4 Mixed traffic scenario of TVs, CV-LCs, and CV-HCs

Figure 16 illustrates the impact of the best and the worst spatial arrangements on the average flow and the average speed of the mixed traffic of TVs, CV-LCs, and CV-HCs. The benefits of the best spatial arrangement can be witnessed in terms of the higher flow and speed in the congested section relative to the worst spatial arrangement. As observed before, the average flow and speed values are in between the best case and the worst case at the congested traffic conditions in the case of random arrangement.

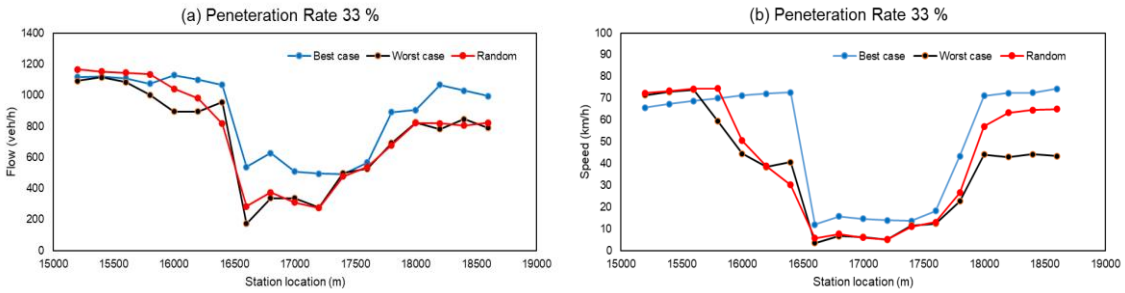

Figure 16 A comparison of fundamental traffic flow parameters among the best, the worst, and the random spatial arrangements of CVs at 33% penetration rate – Scenario TVs, CV-LCs, and CV-HCs. (a) Average flow; and (b) Average speed.

6. STUDY IMPLICATIONS

This research provides valuable contributions to mixed traffic modelling of traditional and connected vehicles. The knowledge of how an efficient distribution of CVs in a traffic stream can enhance traffic flow efficiency, and safety of the mixed traffic of CVs and TVs can assist traffic planners to achieve optimum system goals such as the efficient deployment of CVs, and operation and control of the mixed traffic flow constituting CVs and TVs. Moreover, understanding of how subtle differences in driving behaviour (high compliance and low compliance drivers) impact traffic flow is beneficial at the CV design level, and at planning and policy-making level.

The simulation design and results presented in this study are in line with observations from many CVs field experiments and road trials. For instance, (Farah et al., 2012) investigated the impact of infrastructure-to-vehicle co-operative systems, CO-OPerative SystEms for Intelligent Road Safety (COOPERS), on driver behaviour. A total of 35 participants were recruited in that study, and the safety messages disseminated were speed advice, upstream accident advice, road conditions ahead, lane-keeping advice, and speed limit advice. They reported increased following gaps between the drivers and the vehicle in front and hence enhanced safety. The model utilised in our study to describe the car-following behaviour of connected vehicles can successfully produce such driving behaviours. Michigan connected vehicle testbed trial was one of the first proof-of-concept trials where data were collected at test sites at Ann Arbor, Michigan, on August 25, 2008 between 16:00 and 23:20. The trial included 52 roadside equipment stations and 27 connected vehicles fitted with on-board equipment and DSRC. The basic safety messages were transmitted using on-board equipment. A study by (F. Zhu and Ukkusuri, 2017) reports short oscillation periods of these CVs with narrow oscillation ranges. In our study we also observe short oscillation durations and low oscillation amplitudes for all the simulated homogenous and mixed traffic scenarios involving CVs (particularly for the best case arrangement).

One may argue that it is difficult to assume a connected system without automation (as in this study). We are aware that there are different schools of thought in terms of vehicle connectivity and automation: which will come first, which will dominate, etc. While these are questions still open to debate, connected vehicle technology at its basic level is already available in the real-

world. For example, Google Maps provides you the direction between an origin and a destination, current and future traffic, speed limit information etc., using a combination of GPS satellites, ground station, and a receiver. We can classify such communication in vehicle-to-infrastructure communication category. According to a survey in the year 2018, 77% of smartphone owners use navigation apps and out of these 67% use google maps on a daily basis ("Mobile App Usage Statistics 2018 | The Manifest," 2018). We believe drivers will soon receive information about the leading vehicle as well (such as leading vehicle's speed or distance to the leading vehicle) via navigation apps, and with that high penetration level of navigation apps, policymakers and practitioners shall be ready to accommodate its impact on traffic flow. In developing countries like India, the connected car solutions market is booming with major industries already collaborating to launch affordable connected car devices/onboard diagnostic devices. If the IoT is leveraged adequately, the results and findings from this study will be beneficial.

Similarly, in the future CVs may be equipped with the onboard sensors. Relaxing this study's assumption and considering the effect of onboard sensors can be treated as a fixed effect added across the scenarios and specifically, platoon policies. Though the flow disturbance will decrease, efficiency will increase, and safety will enhance, the disparity among the best case, the worst case, and the random case will be similar.

Indeed, connected and automated vehicles are the future. However, there is still a long way to go before connected and automated vehicles can become the mainstream. Even in the era of connected and automated vehicles, we believe that the manual driving mode will not be eliminated completely for a certain period of time in order to give the driver (or passenger for lack of a better term) the option to take over the vehicle in emergencies. Previous studies have demonstrated that an informed driver is a better decision-maker (Sharma et al., 2020, 2019b). Hence, manual mode with real-time driver assistance (thus, connected vehicles) can be a great option for drivers.

7. CONCLUSIONS AND FUTURE WORK

This study models the mixed traffic of connected vehicles and traditional vehicles using connected vehicle driving strategy integrated with intelligent driver model and intelligent driver model with estimation errors, respectively, and investigates the traffic flow disturbance (measured in terms of oscillation duration and oscillation amplitude), safety (measured in terms of modified time-to-collision and deceleration rate to avoid crash, and efficiency (measured in terms of average flow and average speed) of the resultant mixed traffic environment. Two classes of drivers are considered in connected vehicles, namely high compliance and low compliance drivers. A total of seven mixed traffic environments are generated via different combinations of traditional vehicles, connected vehicles with low compliance drivers, and connected vehicles with high compliance drivers. In addition, this study explores how spatial arrangements of connected vehicles in the mixed traffic platoon influence traffic flow disturbance, efficiency, and safety at varying penetration levels of connected vehicles.

The primary conclusion is that the best spatial arrangement (maximizing the benefits of connected vehicles) of connected vehicles in the platoon will lead to low magnitudes of

oscillation duration and oscillation amplitude, and high values of modified time-to-collision and low values of deceleration rate to avoid crash even at low penetration rates of connected vehicles. On the other hand, the worst spatial arrangement (minimizing the benefits of connected vehicles) of connected vehicles in the platoon, even at high penetration rates of connected vehicles, will lead to high magnitudes of oscillation duration and oscillation amplitude, and low values of modified time-to-collision and high values of deceleration rate to avoid crash. It is observed that, overall, connected vehicles with high compliance and connected vehicles with low compliance platoons both have benefits over traditional vehicles platoon. Among connected vehicles with high compliance and connected vehicles with low compliance platoons, clearly connected vehicles with high compliance class is the winner. In the case of homogenous platoons, it is observed that high compliance drivers drive more efficiently and are at a lower risk than low compliance drivers. Moreover, the flow rate and the average speed is the highest for the platoon with high compliance drivers. In the case of mixed traffic, platoon with connected vehicles with high compliance drivers offer short oscillation duration, low oscillation amplitude, high minimum modified time-to-collision, low deceleration rate to avoid crash, and high average flow and average speed over platoon with connected vehicles with low compliance drivers. Moreover, this study computes traffic efficiency measures such as the average flow and the average speed using the trajectory data. Results from all the mixed traffic environments reveal higher average flow and speed values in case of the best spatial arrangement compared to the worst spatial arrangement. Interestingly, from all the mixed traffic scenarios, under uncongested traffic conditions, the average flow and average speed are high for traditional vehicles platoon as compared to connected vehicles with high compliance and connected vehicles with low compliance platoons. The reason behind this is the large time gap maintained by high compliance and low compliance drivers. Previous studies conjectured that a platoon of connected vehicles result in the high average flow and average speed throughout which is contrary to what we have obtained. Findings from this study underscore that connected vehicles can enhance traffic flow efficiency, and safety; however, traffic engineers and policy makers have to be cautious regarding how connected vehicles are distributed in a traffic stream when deploying these vehicles in the real world traffic environment.

This study assumes a single lane facility in both the experiments to avoid lane-changing events. One of the main objectives of this study is to understand the impact of the spatial distribution of connected vehicles in the platoon on traffic disturbances, efficiency, and safety. If lane-changing events had been added, then it would be difficult to discern whether the changes in traffic disturbances, efficiency, and safety are due to a spatial distribution or due to lane-changing. Based on this study, now it is clear how different spatial distributions of connected vehicles influence traffic disturbances, efficiency, and safety. Thus, future studies can extend our experiments to a multi-lane facility and include lane changing behaviour (Zheng 2014) via connected vehicles lane changing decision models (Ali et al., 2019; Talebpour et al., 2015). Moreover, defining the best and the worst spatial arrangements in the case of the multi-lane facility, and examining traffic flow disturbance, efficiency, and safety in these cases can be important for transitioning to the era of connected and automated vehicles. Another topic worth

researching is developing and assessing the strategies that help connected vehicles to form the best case platoons in the mixed traffic.

Meanwhile, this study assumes perfect communication between the two connected vehicles; however, in real-world, communication impairments such as communication delay and communication loss are unavoidable. Hence, how communication impairments could impact the efficiency, and safety of the mixed traffic of connected and traditional vehicles is an important question to investigate. Information overload, cognitive delays in interpreting and reacting to information, drivers' trust in the technology and its impact on driving behaviour, etc., are some other important aspects that need further investigation. Generic and importantly human factors based multilevel modelling and simulation frameworks proposed by (Calvert et al., 2020; van Lint and Calvert, 2018) can be extended to include above human factors. Furthermore, since traffic hysteresis is an inseparable part of traffic oscillations, future studies can focus on analysing traffic hysteresis (Chen et al., 2012; Saifuzzaman et al., 2017; Zhang, 1999) in the mixed traffic scenarios considering the best and the worst spatial arrangements of connected vehicles at a given penetration rate.

ACKNOWLEDGEMENTS

The authors would like to thank Mr Andrew Haines for programming the simulator experiment and Dr Yasir Ali and Dr Mohammad Saifuzzaman for their help in the experiment design and data collection. This research was partially funded by the Australian Research Council (ARC) through Dr Zuduo Zheng's Discovery Early Career Researcher Award (DECRA; DE160100449).

REFERENCES

Ali, Y., Sharma, A., Haque, Md. M., Zheng, Z., Saifuzzaman, M., 2020. The impact of the connected environment on driving behavior and safety: A driving simulator study. Accid. Anal. Prev. 144, 105643.

Ali, Y., Zheng, Z., Haque, Md. M., Wang, M., 2019. A game theory-based approach for modelling mandatory lane-changing behaviour in a connected environment. Transp. Res. Part C Emerg. Technol. 106, 220–242.

Almqvist, S., Hyden, C., Risser, R., 1991. Use of speed limiters in cars for increased safety and a better environment. Transp. Res. Rec.

Arem, B. van, Driel, C.J.G. van, Visser, R., 2006. The Impact of Cooperative Adaptive Cruise Control on Traffic-Flow Characteristics. IEEE Trans. Intell. Transp. Syst. 7, 429–436.

Arnaout, G.M., Arnaout, J.-P., 2014. Exploring the effects of cooperative adaptive cruise control on highway traffic flow using microscopic traffic simulation. Transp. Plan. Technol. 37, 186–199.

Bhavsar, P., Das, P., Paugh, M., Dey, K., Chowdhury, M., 2017. Risk Analysis of Autonomous Vehicles in Mixed Traffic Streams. Transp. Res. Rec. 2625, 51–61.

Brilon, W., Geistefeldt, J., Regler, M., 2005. Reliability of freeway traffic flow: a stochastic concept of capacity. Presented at the Proceedings of the 16th International symposium on transportation and traffic theory, College Park Maryland.

Calvert, S.C., van Arem, B., van Lint, J.W.C., 2020. A generic multi-level framework for microscopic traffic simulation with automated vehicles in mixed traffic. Transportation Research Part C: Emerging Technologies 110, 291–311.

Cassidy, M.J., Coifman, B., 1997. Relation among average speed, flow, and density and analogous relation between density and occupancy. Transportation Research Record 1591, 1–6.

Chen, D., Ahn, S., Chitturi, M., Noyce, D.A., 2017. Towards vehicle automation: Roadway capacity formulation for traffic mixed with regular and automated vehicles. Transp. Res. Part B Methodol. 100, 196–221.
Chen, D., Laval, J.A., Ahn, S., Zheng, Z., 2012. Microscopic traffic hysteresis in traffic oscillations: A behavioral perspective. Transp. Res. Part B Methodol. 46, 1440–1453.
Chen, Z., He, F., Yin, Y., Du, Y., 2017. Optimal design of autonomous vehicle zones in transportation networks. Transp. Res. Part B Methodol. 99, 44–61.
Ciuffo, B., Casas, J., Montanino, M., Perarnau, J., Punzo, V., 2013. Gaussian process metamodels for sensitivity analysis of traffic simulation models. Transp. Res. Rec. 2390, 87–98.
da Rocha, T. V., Leclercq, L., Montanino, M., Parzani, C., Punzo, V., Ciuffo, B., Villegas, D., 2015. Does traffic-related calibration of car-following models provide accurate estimations of vehicle emissions? Transp. Res. Part D 34, 267–280.
Edie, L., 1963. Discussion on Traffic Stream Measurements and Definitions. Presented at the Proc. 2nd International Symposium of the Theory of Trafiic Flow, Paris, France.
Farah, H., Koutsopoulos, H.N., Saifuzzaman, M., Kölbl, R., Fuchs, S., Bankosegger, D., 2012. Evaluation of the effect of cooperative infrastructure-to-vehicle systems on driver behavior. Transportation Research Part C: Emerging Technologies 21, 42–56.
Fernandes, P., Nunes, U., 2012. Platooning With IVC-Enabled Autonomous Vehicles: Strategies to Mitigate Communication Delays, Improve Safety and Traffic Flow. IEEE Trans. Intell. Transp. Syst. 13, 91–106.
Friedrich, B., 2016. The effect of autonomous vehicles on traffic, in: Autonomous Driving. Springer, pp. 317–334.
Ghiasi, A., Hussain, O., Qian, Z., Li, X., 2017. A mixed traffic capacity analysis and lane management model for connected automated vehicles: A Markov chain method. Transp. Res. Part B Methodol. 106, 266–292.
Gipps, P.G., 1981. A behavioural car-following model for computer simulation. Transp. Res. Part B Methodol. 15, 105–111.
Gong, S., Du, L., 2018. Cooperative platoon control for a mixed traffic flow including human drive vehicles and connected and autonomous vehicles. Transp. Res. Part B Methodol. 116, 25–61.
Gu, Z., Saberi, M., 2019. Effects of Turning and Merging on Network Traffic Instability: A Simulation-Based Analysis of Human-Driven and Autonomous Vehicles. arXiv:1904.11677 [cs, math].
Guériau, M., Billot, R., El Faouzi, N.-E., Monteil, J., Armetta, F., Hassas, S., 2016. How to assess the benefits of connected vehicles? A simulation framework for the design of cooperative traffic management strategies. Transp. Res. Part C Emerg. Technol. 67, 266–279.
Jerath, K., Brennan, S.N., 2012. Analytical Prediction of Self-Organized Traffic Jams as a Function of Increasing ACC Penetration. IEEE Trans. Intell. Transp. Syst. 13, 1782–1791.
Jia, D., Ngoduy, D., 2016. Enhanced cooperative car-following traffic model with the combination of V2V and V2I communication. Transp. Res. Part B Methodol. 90, 172–191.
Jia, D., Ngoduy, D., Vu, H.L., 2019. A multiclass microscopic model for heterogeneous platoon with vehicle-to-vehicle communication. Transp. B Transp. Dyn. 7, 448–472.
Jiang, H., Hu, J., An, S., Wang, M., Park, B.B., 2017. Eco approaching at an isolated signalized intersection under partially connected and automated vehicles environment. Transp. Res. Part C Emerg. Technol. 79, 290–307.
Kahneman, D., Tversky, A., 1979. Prospect theory: An analysis of decision under risk. Econom. J. Econom. Soc. 263–291.
Kesting, A., Treiber, M., Schönhof, M., Helbing, D., 2008. Adaptive cruise control design for active congestion avoidance. Transp. Res. Part C Emerg. Technol. 16, 668–683.
Kim, T., 2015. Assessment of Vehicle-to-Vehicle Communication based Applications in an Urban Network (PhD). Virginia Polytechnic Institute and State University, Blacksburg, VA.
Levin, M.W., Boyles, S.D., 2016. A multiclass cell transmission model for shared human and autonomous vehicle roads. Transp. Res. Part C Emerg. Technol. 62, 103–116.
Liu, H., Kan, X. (David), Shladover, S.E., Lu, X.-Y., Ferlis, R.E., 2018. Modeling impacts of Cooperative Adaptive Cruise Control on mixed traffic flow in multi-lane freeway facilities. Transp. Res. Part C Emerg. Technol. 95, 261–279.
Liu, H., Wei, H., Zuo, T., Li, Z., Yang, Y.J., 2017. Fine-tuning ADAS algorithm parameters for optimizing traffic safety and mobility in connected vehicle environment. Transp. Res. Part C Emerg. Technol. 76, 132–149.

Mobile App Usage Statistics 2018 | The Manifest [WWW Document], 2018. URL https://themanifest.com/mobile-apps/mobile-app-usage-statistics-2018 (accessed 8.6.20).
Newell, G.F., 2002. A simplified car-following theory: a lower order model. Transp. Res. Part B Methodol. 36, 195–205.
Ngoduy, D., 2012. Application of gas-kinetic theory to modelling mixed traffic of manual and ACC vehicles. Transportmetrica 8, 43–60.
Ni, D., Leonard, J.D., 2006. Direct Methods of Determining Traffic Stream Characteristics by Definition. Presented at the 85th Annual Meeting Transportation Research Board. Washington, DC.
Ni, D., Li, J., Andrews, S., Wang, H., 2011. A Methodology to Estimate Capacity Impact due to Connected Vehicle Technology. Int. J. Veh. Technol. 2012, e502432.
Olia, A., Abdelgawad, H., Abdulhai, B., Razavi, S.N., 2016. Assessing the Potential Impacts of Connected Vehicles: Mobility, Environmental, and Safety Perspectives. J. Intell. Transp. Syst. 20, 229–243.
Ossen, S., Hoogendoorn, S.P., 2011. Heterogeneity in car-following behavior: Theory and empirics. Transp. Res. Part C Emerg. Technol.19, 182–195.
Ozbay, K., Yang, H., Bartin, B., Mudigonda, S., 2008. Derivation and validation of new simulation-based surrogate safety measure. Transportation research record 2083, 105–113.
Punzo, V., Montanino, M., 2016. Speed or spacing? Cumulative variables, and convolution of model errors and time in traffic flow models validation and calibration. Transp. Res. Part B 91, 21–33.
Rahman, M.S., Abdel-Aty, M., 2018. Longitudinal safety evaluation of connected vehicles' platooning on expressways. Accid. Anal. Prev. 117, 381–391.
Rahman, M.S., Abdel-Aty, M., Wang, L., Lee, J., 2018. Understanding the Highway Safety Benefits of Different Approaches of Connected Vehicles in Reduced Visibility Conditions. Transp. Res. Rec. 0361198118776113.
Rao, B.S.Y., Varaiya, P., 1993. Flow benefits of autonomous intelligent cruise control in mixed manual and automated traffic. Transp. Res. Rec. 1408, 36–43.
Rios-Torres, J., Malikopoulos, A.A., 2018. Impact of Partial Penetrations of Connected and Automated Vehicles on Fuel Consumption and Traffic Flow. IEEE Trans. Intell. Veh. 3, 453–462.
Saifuzzaman, M., Zheng, Z., 2014. Incorporating human-factors in car-following models: A review of recent developments and research needs. Transp. Res. Part C Emerg. Technol. 48, 379–403.
Saifuzzaman, M., Zheng, Z., Haque, M.M., Washington, S., 2017. Understanding the mechanism of traffic hysteresis and traffic oscillations through the change in task difficulty level. Transp. Res. Part B Methodol. 105, 523–538.
Schakel, W.J., Arem, B. van, Netten, B.D., 2010. Effects of Cooperative Adaptive Cruise Control on traffic flow stability. Presented at the 13th International IEEE Conference on Intelligent Transportation Systems, 759–764.
Sharma, A., Ali, Y., Saifuzzaman, M., Zheng, Z., Haque, M.M., 2017. Human Factors in Modelling Mixed Traffic of Traditional, Connected, and Automated Vehicles, in: Advances in Human Factors in Simulation and Modeling, Advances in Intelligent Systems and Computing. Springer, Cham, pp. 262–273.
Sharma, A., Zheng, Z., Bhaskar, A., 2019a. Is more always better? The impact of vehicular trajectory completeness on car-following model calibration and validation. Transp. Res. Part B Methodol. 120, 49-75.
Sharma, A., Zheng, Z., Bhaskar, A., Haque, Md.M., 2019b. Modelling car-following behaviour of connected vehicles with a focus on driver compliance. Transp. Res. Part B Methodol. 126, 256–279.
Sharma, A., Zheng, Z., Kim, J., Bhaskar, A., Haque, Md.M., 2019c. Estimating and Comparing Response Times in Traditional and Connected Environments. Transp. Res. Rec. 2673, 674-684.
Sharma, A., Zheng, Z., Kim, J., Bhaskar, A., Haque, M.M., 2020. Is an informed driver a better decision maker? A grouped random parameters with heterogeneity-in-means approach to investigate the impact of the connected environment on driving behaviour in safety-critical situations. Anal. Methods Accid. Res. 27, 100127.
Shladover, S.E., Su, D., Lu, X.-Y., 2012. Impacts of Cooperative Adaptive Cruise Control on Freeway Traffic Flow. Transp. Res. Rec. 2324, 63–70.
Sommer, C., German, R., Dressler, F., 2011. Bidirectionally Coupled Network and Road Traffic Simulation for Impr9oved IVC Analysis. IEEE Trans. Mob. Comput. 10, 3–15.
Talebpour, A., Mahmassani, H., Hamdar, S., 2011. Multiregime Sequential Risk-Taking Model of Car-Following Behavior: Specification, Calibration, and Sensitivity Analysis. Transp. Res. Rec. J. Transp. Res. Board 60–66.

Talebpour, A., Mahmassani, H.S., 2016. Influence of connected and autonomous vehicles on traffic flow stability and throughput. Transp. Res. Part C Emerg. Technol. 71, 143–163.
Talebpour, A., Mahmassani, H.S., Bustamante, F.E., 2016. Modeling Driver Behavior in a Connected Environment. Transp. Res. Rec. J. Transp. Res. Board 2560, 75–86.
Talebpour, A., Mahmassani, H.S., Elfar, A., 2017. Investigating the Effects of Reserved Lanes for Autonomous Vehicles on Congestion and Travel Time Reliability. Transp. Res. Rec. 2622, 1–12.
Talebpour, A., Mahmassani, H.S., Hamdar, S.H., 2015. Modeling Lane-Changing Behavior in a Connected Environment: A Game Theory Approach. Transp. Res. Procedia, 21st International Symposium on Transportation and Traffic Theory Kobe, Japan, 5-7 August, 2015 7, 420–440.
Treiber, M., Hennecke, A., Helbing, D., 2000. Congested traffic states in empirical observations and microscopic simulations. Phys. Rev. E 62, 1805–1824.
Treiber, M., Kesting, A., 2013. Traffic flow dynamics. Traffic Flow Dyn. Data Models Simul. Springer-Verl. Berl. Heidelb.
Treiber, M., Kesting, A., Helbing, D., 2006. Delays, inaccuracies and anticipation in microscopic traffic models. Phys. Stat. Mech. Its Appl. 360, 71–88.
van den Berg, V.A.C., Verhoef, E.T., 2016. Autonomous cars and dynamic bottleneck congestion: The effects on capacity, value of time and preference heterogeneity. Transp. Res. Part B Methodol. 94, 43–60.
van Lint, J.W.C., Calvert, S.C., 2018. A generic multi-level framework for microscopic traffic simulation—Theory and an example case in modelling driver distraction. Transp. Res. Part B Methodol. 117, 63–86.
Vander Werf, J., Shladover, S.E., Miller, M.A., Kourjanskaia, N., 2002. Effects of Adaptive Cruise Control Systems on Highway Traffic Flow Capacity. Transp. Res. Rec. 1800, 78–84.
Vogel, K., 2003. A comparison of headway and time to collision as safety indicators. Accid. Anal. Prev. 35, 427–433.
Wang, M., Daamen, W., Hoogendoorn, S.P., Arem, B. van, 2016. Connected variable speed limits control and car-following control with vehicle-infrastructure communication to resolve stop-and-go waves. J. Intell. Transp. Syst. 20, 559–572.
Wang, M., Treiber, M., Daamen, W., Hoogendoorn, S.P., van Arem, B., 2013. Modelling supported driving as an optimal control cycle: Framework and model characteristics. Transp. Res. Part C Emerg. Technol. 36, 547–563.
Xie, D., Zhao, X., He, Z., 2018. Heterogeneous Traffic Mixing Regular and Connected Vehicles: Modeling and Stabilization. IEEE Trans. Intell. Transp. Syst. 1–12.
Ye, L., Yamamoto, T., 2018. Modeling connected and autonomous vehicles in heterogeneous traffic flow. Phys. Stat. Mech. Its Appl. 490, 269–277.
Zhang, H.M., 1999. A mathematical theory of traffic hysteresis. Transp. Res. Part B Methodol. 33, 1–23.
Zhao, L., Malikopoulos, A., Rios-Torres, J., 2018. Optimal Control of Connected and Automated Vehicles at Roundabouts: An Investigation in a Mixed-Traffic Environment. 15th IFAC Symposium on Control in Transportation Systems CTS 2018 51, 73–78.
Zheng, L., Sayed, T., 2019. Comparison of Traffic Conflict Indicators for Crash Estimation using Peak Over Threshold Approach. Transp. Res. Rec. 2673, 493–502.
Zheng, L., Sayed, T., Essa, M., 2019. Validating the bivariate extreme value modeling approach for road safety estimation with different traffic conflict indicators. Accid. Anal. Prev. 123, 314–323.
Zheng, Z., 2014. Recent developments and research needs in modeling lane changing. Transp. Res. Part B Methodol. 60, 16-32.
Zheng, Z., Ahn, S., Chen, D., Laval, J., 2011. Applications of wavelet transform for analysis of freeway traffic: Bottlenecks, transient traffic, and traffic oscillations. Transp. Res. Part B Methodol. 45, 372–384.
Zheng, Z., Ahn, S., Chen, D., Laval, J., 2013. The effects of lane-changing on the immediate follower: Anticipation, relaxation, and change in driver characteristics. Transp. Res. Part C Emerg. Technol. 26, 367-379.
Zheng, Z., Washington, S., 2012. On selecting an optimal wavelet for detecting singularities in traffic and vehicular data. Transp. Res. Part C Emerg. Technol. 25, 18–33.
Zhu, F., Ukkusuri, S.V., 2017. Modeling the Proactive Driving Behavior of Connected Vehicles: A Cell-Based Simulation Approach. Comput.-Aided Civ. Infrastruct. Eng. 33, 262–281.
Zhu, F., Ukkusuri, S.V., 2016. An Optimal Estimation Approach for the Calibration of the Car-Following Behavior of Connected Vehicles in a Mixed Traffic Environment. IEEE Trans. Intell. Transp. Syst. PP, 1–10.